Mechanistic Aspects of Maleic Anhydride Synthesis from C_4 Hydrocarbons over Phosphorus Vanadium Oxide

GABRIELE CENTI and FERRUCCIO TRIFIRÒ

Department of Industrial Chemistry and Materials, University of Bologna, Bologna, Italy

JERRY R. EBNER* and VICTORIA M. FRANCHETTI

Monsanto Chemical Company, St. Louis, Missouri 63167

Contents

I. Introduction

A. Background

Maleic anhydride (2,5-furandione) and its derivatives (malic and fumaric acids) are produced with a worldwide capacity of about 1300 million pounds per year. The demand for this industrially important chemical, used principally in the manufacture of unsaturated polyester resins, agricultural chemicals, food additives, lubricating oil additives, and pharmaceuticals,[1-3] is expected to grow over the next 5 years, due in part to new uses for this highly functionalized molecule. Among the more significant potential new uses is its conversion to butanediol via hydrogenation of maleic acid. This chemistry may become economically more favorable than the present acetylene-based chemistry by the 1990s.[4-6]

Currently, worldwide production of maleic anhydride is based on the major feedstocks benzene, n-butane, and butenes.[7-12] Most of the capacity is produced via fixed-bed oxidation of benzene, though benzene is being displaced by butane as a feedstock (all production in the U.S. is butane based), because butane is a lower cost and environmentally more desirable raw material and because butane oxidation produces a cleaner product stream, forming mainly maleic anhydride and carbon oxides. However, productivity from n-butane is lower due to lower selectivities to maleic anhydride at higher conversions and the somewhat lower feed concentrations (less than 2 molar %) used to avoid flammability of process streams.

A survey of the patent literature indicates molar selectivities for fixed-bed production of maleic anhydride from butane of around 67–75% under typical "industrial" conditions (less than 2 molar % butane, conversion from 70 to 85% between 400 and 450 °C, and space velocities of around 1100–2600 h⁻¹).[13-18] In the past few years, development of fluid bed butane-based systems has been reported.[19,20] These systems offer the advantage of operation at higher butane concentrations (up to 4%) and thus lower original capital costs. However, loss in selectivity at the higher butane loadings and the inherent problems with attrition of phosphorus vanadium oxide (PVO) materials need to be overcome before this process will become economically preferred. The recently developed DuPont transport bed technology may be the most economically favorable route for maleic production in the 1990s. This process operates at lower conversions per pass and with higher selectivities than normally encountered in fixed or fluid bed systems, and uses a unique attrition resistance system.[21,22]

All catalysts used industrially for the production of maleic anhydride from butane are PVO-based systems.[12,23-25] The preparation of vanadium phosphorus oxides was the subject of a recent review by Hodnett,[24] and older data on these catalysts have been reviewed by Varma and Saraf[12] and by Hucknall.[25] The vanadium phosphorus oxide system is characterized by facile formation and interconversion of a number of crystalline V(IV) and V(V) phases, and this has led to some confusion in the literature as to the nature of the active phase.[23] In the PVO system, there are many synthesis variables that affect the solid-state chemistry leading to the active catalyst, and thus the performance char-

Gabriele Centi was born in Bolzano, Italy, and graduated from the University of Bologna (Italy) in 1979. After completing his post-doctoral work at the Experimental Station for Fuels (Italy), he moved to the University of Bologna, where he is presently a Professor of Chemical Engineering. His main research interests are in the catalytic, synthetic, and engineering aspects of selective oxidation reactions, in particular on the relationship between solid-state and surface aspects and mechanistic aspects of catalysis on mixed and supported oxides.

Ferruccio Trifirò is Full Professor in Industrial Chemistry at the University of Bologna (Italy) and took his degree in chemical engineering from the Politecnico Milano (Italy) in 1963, working there until 1974. He was a postdoctoral fellow at the Hievrosky Institute (Czechoslovakia) and at the University of Reading (United Kingdom) and Visiting Professor at the University of Erlangen (Germany). He is presently President of the Catalysis Group of the Italian Chemistry Society and Director of the Department of Industrial Chemistry and Materials of the University of Bologna. His main interests are in heterogeneous chemistry, solid-state and surface characterization, catalytic tests, and kinetic and mechanistic aspects. He holds several patents in heterogeneous oxidation processes. His interests also include photooxidation reactions and the relationship between homogeneous and heterogeneous mechanisms.

Jerry Ebner is a Monsanto Science Fellow, Catalyst Technology. Born in LaCrosse, WI, he obtained his Ph.D. in inorganic chemistry at Purdue University in 1975 under Professor R. A. Walton. He has conducted research in the field of heterogeneous catalysis since he joined Monsanto Chemical Co. in 1975. Since 1982 he has served as group leader of heterogeneous catalysis in the selective oxidation and ammoxidation areas, as well as group leader of the corporate catalysis research group. In 1986 he was appointed a Monsanto Science Fellow. His research interests include new catalyst synthesis and characterization, solid-state chemistry, and studies of chemical surface reactions through the development and application of new catalyst characterization methods.

Victoria Franchetti presently is Director of Research, Plastic Technology, Monsanto Chemical Co. From 1984 to 1987 she was Manager, Maleic Catalyst Technology, within the Specialty Chemical Division. She received her Ph.D. from Boston University in 1975 and joined Monsanto Chemical Co. in 1977 after completing a 2-year postdoctoral appointment at Purdue University. Her research and management experience at Monsanto has included the areas of solid characterization, process analytical development, catalysis, and new plastics technology.
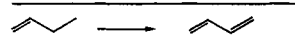
acteristics and mechanism of catalysis. For example, the use of an organic solvent during preparation as opposed to an aqueous system results in differing degrees of crystallinity[26] and defect structure of the resulting active phase. The final P:V ratio of the active phase may be varied and has been the subject of numerous publications.[27-60]

However, recent advances in understanding the solid-state chemistry of PVO have allowed studies of this reaction with well-characterized, reproducible compositions. This has resulted in better analysis of the role of oxidation states, the P:V ratio, and defect structure on the reaction mechanism.

B. Scope of the Review

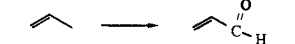The n-butane to maleic anhydride reaction is a fascinating and complex system. This catalytic system performs a 14-electron oxidation involving the abstraction of 8 hydrogen atoms and insertion of 3 oxygen atoms (eq 1). Compared to other industrially practiced

$$C_4H_{10} + 3.5 O_2 \longrightarrow \text{[maleic anhydride]} + 4 H_2O \tag{1}$$
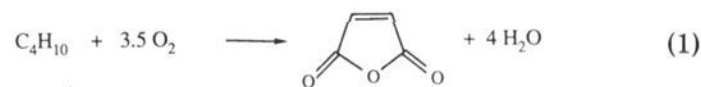
hydrocarbon selective oxidation reactions,[61-67] it is the most complex (Table I). It is the only example of an industrially practiced selective oxidation reaction involving alkane activation. Knowledge gained through study and understanding of this system may contribute to advances in alkane activation in general.

The subject of this review is a critical analysis of data published in recent years concerning the mechanism of the oxidation of n-butane with vanadium phosphorus oxide catalysts. We will present an overall general picture of this mechanism and clarify issues related to the nature of the active site involved, including the

TABLE 1. Number of Electrons and Oxygen Molecules Involved in the Principal Reactions of Industrial Interest in Selective Oxidation

REACTION		ELECTRONS INVOLVED	MOLES OXYGEN
(propene → acrolein) + H₂O		2	0.5
(ethylene → ethylene oxide) + H₂O		4	1
(propene → acrolein) + H₂O		4	1
(o-xylene → phthalic anhydride) + 3 H₂O		12	3
(butene → maleic anhydride) + 4 H₂O		14	3.5

importance of P:V ratio, oxidation state, structural characteristics of the vanadium phosphorus oxide system, and the detection and formation of intermediates.

One characteristic of the n-butane reaction is the absence of "observed" intermediates during steady-state oxidation, as compared to the oxidation of 1-butene, for example.[59,68,69] Kinetic studies have been of little value in determining reaction sequences because the rate-determining step[70] is alkane activation. In order to detect intermediates, conditions preventing the further oxidation of these intermediates must be chosen. We will analyze how these intermediates are formed and discuss recent insight generated from a new technique, temporal analysis of products (TAP).[71,72] The reaction sequences may be determined by using controlled conditions and TAP.

Another characteristic of the selective oxidation of butane involves the series of oxidation steps utilizing different kinds and reactivities of oxygen. We will review the experimental work relevant to determination of the forms of selective and nonselective oxygen in the reaction, addressing the question of whether the Mars and van Krevelen redox mechanism common to olefin oxidation[61-67] applies equally well to this saturated system.

Heterogeneous catalysis is a science at the interface of different areas of chemistry, physical chemistry, and engineering. Each new development stems from applications of concepts from these different areas. A heterogeneous catalytic system should be, in fact, correctly regarded as a three-phase system: (i) a gas phase, (ii) a solid phase, and (iii) a two-dimensional surface region at the gas-solid interface composed of the surface solid phases and interacting adsorbed molecules.[63] The structure and properties of this surface region may be modified either by changing the composition of the gas phase or by altering the properties of the solid. A further objective of this review is, therefore, to illustrate how only a global interdisciplinary approach allows increased understanding of complex reaction systems.

II. Structure of the Catalyst

A. Crystalline PVO Phases

The vanadium phosphorus oxide system is characterized by the facile formation of a number of crystalline

phases, both of vanadium(IV) and of vanadium(V). In the more interesting P:V atomic ratio near 1.0, the different crystalline (α, β),[50,74-82] polymorphic (α_I, α_{II}, γ, δ),[31-33,80-82] or hydrated phases of $VOPO_4$[31-33,50,74-87] have been extensively studied. In general, the vanadyl orthophosphate crystal structure consists of VO_6 and PO_4 groups arranged in layers $[VOPO_4]_\infty$, held together by long V–O bonds or by hydrogen bonds. The layered structure leads to a rich intercalation chemistry, with formation of layered solids consisting of alternating inorganic and organic layers[88] or the formation of solvated inorganic intercalation compounds.[89,90]

In dihydrated $VOPO_4$ the layer lattice is built up of neutral $VOPO_4$ layers and interlayer water molecules.[85-87] The vanadium atom lies on a fourfold axis and is surrounded by six oxygen atoms to give a distorted octahedron. The four equatorial oxygens are provided by four different phosphate tetrahedra. One of the axial vanadium–oxygen bond distances is very short, corresponding to a vanadium–oxygen double bond (V=O). The structure of α-$VOPO_4$ is composed of chains of highly distorted VO_6 octahedra sharing four oxygen atoms with four different PO_4 groups.[74-82] These groups are arranged to form layers. A distortion of the VO_6 octahedra occurs along the c axis, generating a short V–O bond (V=O) and a very long V–O bond (V⋯O). Thus the oxyvanadium units can be approximated as VO_5 pyramids. The β-$VOPO_4$ phase possesses VO_5 pyramids and PO_4 tetrahedra in its crystal structure, analogous to α-$VOPO_4$. However, the primitive unit cell of β-$VOPO_4$ contains twice the number of such structural groups, resulting in a network structure. The γ- and δ-polymorphic forms of $VOPO_4$ are suggested[31-33,73] to contain a different framework, in which pairs of edge-sharing octahedra with trans vanadyl oxygens are alternately unshared or shared with phosphate tetrahedra. Such pairs do not exist in the α- and β-$VOPO_4$ forms. During thermal treatment at high temperature the consecutive transitions

$$\delta\text{-}VOPO_4 \xrightarrow{\Delta} \gamma\text{-}VOPO_4 \xrightarrow{\Delta} \beta\text{-}VOPO_4 \qquad (2)$$
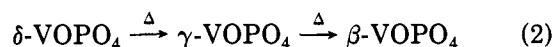
have been observed.[33]

Vanadium(IV) hydrogen phosphate,[91-94] which is the most widely used precursor of the active phase for n-butane oxidation,[22,31,58-60,91-96] possesses a structure made up of atom arrangements in the ac plane which are very similar to that proposed for γ-$VOPO_4$. It may be obtained from the dihydrated V(V) phosphate by reduction with organic alcohols[91] or from the reduction of V_2O_5 followed by o-H_3PO_4 addition.[58-60,95,96] Both the hemihydrate and tetrahydrate of vanadium hydrogen phosphate are known,[92] and their structures are closely related, showing a layered structure and pairs of face-sharing vanadium(IV) octahedra. Hydrogen phosphate (OH) groups are directed into the interlayer space. The coordination geometry around both vanadium and phosphorus is similar in the two structures. The possible formation of the trihydrate of $VOHPO_4$ has also been reported.[36] The $VOHPO_4 \cdot 0.5H_2O$ framework is reminiscent of the structures of analogous layered compounds of zirconium hydrogen phosphates and hydrated Nb phosphates. The intercalation compounds of vanadium hydrogen phosphate with organic molecules or inorganic cations and anions such as V^{n+} or HPO_4^{2-}[78,79,95,102,103] are similar to those reported in the
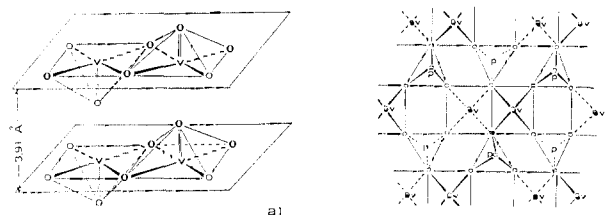
Figure 1. Idealized vanadyl pyrophosphate structure:[26] (a) only vanadyl groups; (b) connectivity of octahedra and tetrahedra within a layer containing the vanadyl dimer groups.

literature for the zirconium and niobium systems.[97-101] This intercalation chemistry is of particular importance in the description of the structural and catalytically related chemistry of $VOHPO_4 \cdot 0.5H_2O$ and of its derived phases. Two main effects observed in the preparation of $VOHPO_4 \cdot 0.5H_2O$ may be, in fact, strictly connected to intercalation properties. First, nonstoichiometry is easily accommodated as evidenced by the preparation of compounds with 0.9–1.2 P:V atomic ratio without any apparent modification of structural and morphological properties.[95] Second, the preparation conditions have a pronounced effect on the microstructure,[22,26,31,95,104-107] i.e., on the morphology, solid-state reactivity, and the presence of disorder in the stacking fold of crystalline planes of its layered structure. In fact, reduction of the starting V^V compound may be realized[96] by using, for example, aqueous HCl or isobutyl alcohol. In both cases, almost pure vanadyl hydrogen phosphate is obtained, but with different microstructures.[96,104-107] The layers of vanadyl hydrogen phosphate ((010) planes) are interconnected in a tridimensional structure by weak H bonding of phosphates and of water molecules. The organic alcohol competes with this effect, reducing the bonding between the planes and allowing the formation of crystals in which these (010) planes are predominantly exposed (platelike morphology).[22,41,91,93,96] This effect, in addition to the increase in surface area,[60] modifies the surface properties due to a change in the relative ratio of crystalline planes at the surface. The alcohol also can remain partially intercalated between layers.[96] This effect induces some local modification of the vanadyl hydrogen phosphate structure, which can strongly modify its solid-state reactivity.[104-107]

The transformation of V(IV) and V(V) phases into vanadyl pyrophosphate is an important step in forming active catalysts. By thermal treatment at ca. 400 °C, the $VOHPO_4 \cdot 0.5H_2O$ dehydrates to $(VO)_2P_2O_7$. Alternatively, the vanadyl pyrophosphate may be obtained by reduction from $VOPO_4$ or by thermal treatment of different crystalline or amorphous P–V–O–X phases (where X indicates a generic thermally decomposable anion or cation such as $C_2O_4^{2-}$ or NH_4^+).[28,36,52,57,58] The vanadyl pyrophosphate is built of chains of V polyhedra linked by pyrophosphate groups.[108,109] The V atoms are linked through the oxygen atoms of the vanadyl in V–O–V chains in the c direction, and the V octahedra are linked in pairs through a common edge, forming double chains in this direction. The vanadyl groups in the paired vanadium octahedra are oriented trans to one another, as schematically represented in Figure 1. The unit cell of $(VO)_2P_2O_7$ is orthorhombic[108,109] and is topologically similar (in its bc plane) to that of $VOHPO_4 \cdot 0.5H_2O$ (in the ab plane).[91,94] The change from face-shared to edge-shared vanadium octahedra in

converting the hemihydrate to the pyrophosphate results in a small expansion of one axis, but the other in-plane dimension shows little change according to the pseudomorphic relations between the two crystalline structures.[93] This indicates a topotactic mechanism of transformation, and this result has been confirmed with scanning electron microscopy.[22,31,91,93,96] The layer spacing decreases from 5.69 Å in the hemihydrate to 3.86 Å in the pyrophosphate. This is consistent with removing the water molecules shared by the vanadium pairs and filling the resulting vanadium coordination site with the oxygen atoms of vanadyl groups from the layer above. This transformation requires only very small displacements of the atoms. Importantly, since the conversion of the hemihydrate to pyrophosphate can take place without breaking any V–O–P bonds, the structural order/disorder and morphology of the precursor phase are maintained during the transformation to vanadyl pyrophosphate. This means that it is possible to control some of the structural/morphological characteristics of vanadyl pyrophosphate by control of the specific nature of the $VOHPO_4 \cdot 0.5H_2O$ precursor phase.[96,105] Furthermore, the terminal vanadyl oxygen atoms in the face-shared octahedra pairs of vanadyl hydrogen phosphate have a syn arrangement, while in vanadyl pyrophosphate they are in anti positions. These arrangements in the layer stacking direction result in the initial formation of $(VO)_2P_2O_7$ crystallites with many defects.[26,106,107,110,111] The possible presence of disorder in the crystalline structure of vanadyl pyrophosphate was confirmed by magnetic susceptibility measurements,[110] and its role in the mechanism of the reaction was suggested.[26,111] Alternatively, Bordes and Courtine[31-33,73] discuss these effects in terms of different crystalline phases (β- and γ-$(VO)_2P_2O_7$), in which the former possesses a network structure versus a layered structure for the γ phase. X-ray diffraction patterns, however, are very similar in these two phases. According to these authors, β-$(VO)_2P_2O_7$ forms with a crystallographic shear mechanism from β-$VOPO_4$, whereas γ-$(VO)_2P_2O_7$ forms by dehydration of vanadyl hydrogen phosphate or reduction from γ-$VOPO_4$.

In addition to these 1:1 phosphorus vanadium compounds, some authors have found the formation of other crystalline phases in catalysts with P:V ratio in the 0.8–2.0 range. In particular, the formation of $VO(H_2PO_4)_2$ in the precursor phase[34,36,112] and $V(PO_3)_3$ and $VO(PO_3)_2$ or other polyphosphates[34,36,50,113] in the activated catalysts was evidenced. These phases, however, were generally considered to be inactive in n-butane oxidation.[24] Finally, poorly crystalline or amorphous PVO phases were sometimes observed in the preparation of these vanadium phosphorus oxide systems.[47,52,54,58,114-119]

B. Active Phase in n-Butane Selective Conversion

Because the vanadium phosphorus oxide system is characterized by the facile formation of a number of crystalline phases, the structure of the active phase must be discussed in terms of factors such as oxidation state, P:V ratio, and crystal phase transformations under reactant atmosphere. The various crystal phases can interconvert as a function of the reducing or oxi-

dizing properties of the reactants, the time on stream, and the reaction temperature.[33,50,58,59,104,106,107,120,121] For this reason, some authors adopted a systematic approach to preparation of these catalysts using statistical design and evaluation of experimental results.[55,122] In this section we examine the important features related to formation of the active phase and the various conclusions that have emerged in the literature concerning the nature of the active phase.

The orthophosphate (VOPO$_4$) phases are transformed to (VO)$_2$P$_2$O$_7$ by reaction with the hydrocarbon mixture. In this reduction process single VO$_6$ octahedra form pairs by loss of oxide anions. However, the different VOPO$_4$ phases previously discussed possess different reducibility to vanadyl pyrophosphate, depending on the structure or morphology.[33,59,73] The constitutive layers of the γ-VOPO$_4$ framework have a tendency[31] to shift cooperatively along the Bürger vector in order to progressively form the columns of edge-share octahedra and pyrophosphate groups of (VO)$_2$P$_2$O$_7$. This transformation is easier than the movement along the crystallographic shear planes proposed to account for the reduction of β-VOPO$_4$.[31,33,73] Also α-VOPO$_4$ reduces[59,104] under less severe conditions compared to those needed to reduce β-VOPO$_4$. However, the α-VOPO$_4$ can also transform to β-VOPO$_4$ at high temperatures, particularly in the hot-spot zones of fixed-bed reactors. The presence of β-VOPO$_4$ in used or inactive catalysts for butane oxidation accounts for a loss of catalytic performance, and its greater stability compared with that of the other forms of VOPO$_4$ limits its further transformation.[33,59]

This complex solid-state chemistry has led to some confusion and contradictions in the literature concerning the nature of the active phase in n-butane oxidation and the identification of the active sites involved in the different steps of the reaction.

Bordes and Courtine[33,123] suggest that the active sites in n-butane oxidation to maleic anhydride are associated with coherent interfaces between slabs of (100) VOPO$_4$ and of (010) (VO)$_2$P$_2$O$_7$ along the (100) and (201) planes, respectively. Volta et al.,[117-119] on the contrary, believe that the active sites are not associated with interfacial effects between two crystalline phases. On the basis of comparison between X-ray diffraction and radial electron distribution data they suggest that the active phase for selective oxidation of n-butane consists of a mixture of well-crystallized (VO)$_2$P$_2$O$_7$ (V^{4+}) and an amorphous surface PVO phase of V^{5+} involving many corner-sharing VO$_6$ octahedra. This amorphous phase may be interpreted as a precursor of β-VOPO$_4$, which forms at higher reaction temperatures. According to Buchanan et al.[114] a methanol washing treatment of the catalysts removes a soluble amorphous V^{5+} species, and this treatment, as opposed to that suggested by Volta et al.,[117-119] improves catalytic performance. A solubilizable amorphous V^{5+}PO$_4$ phase was evidenced also by Centi et al.[58] Buchanan et al.[114] suggest that strongly oxidizing or reducing treatments lead to catalysts with particularly poor selectivity and in situ activation procedures in n-butane/air at reaction temperatures give the best results. However, Hodnett and Delmon[38-40] used a prereduction treatment with hydrogen in order to improve selectivity to maleic anhydride and suggest that the best catalyst consists of an oxidized surface layer built upon a reduced core of

a V^{4+} phase. The selectivity is not related to the presence of a specific well-crystallized phase, but only to the distribution of vanadium oxidation states between the bulk and the surface.

The active catalyst must possess an optimal V^{4+}/V^{5+} ratio for selectivity in n-butane oxidation according to Zazhigalov et al.[103] from studies of V/P–mica compounds with variable V(IV)/V(V) ratios. These compounds preserve the layer structure of the initial α-V^{5+}OPO$_4$ compound. Optimal performance properties are associated with catalysts containing 4–9 V(V) ions per V(IV) ion. The same authors[124-127] have studied the catalytic behavior of α- and β-VOPO$_4$ phases in n-butane oxidation. No significant differences in the activities of the two phases were observed.[127] n-Butane oxidation and maleic anhydride formation take place at the expense of the catalyst surface oxygen and are accompanied by its reduction to vanadyl pyrophosphate. On vanadyl pyrophosphate,[127,128] however, the rate of reduction of the catalyst is lower than that of reaction, and therefore these authors conclude that the V(V) phase is reduced and that the V(IV) phase is oxidized under the dynamic conditions of catalytic reaction. Similar conclusions are reported by Moser and Schrader[113] from a flow reactor study of the effect of oxygen in the selective oxidation of n-butane over β-VOPO$_4$ and (VO)$_2$P$_2$O$_7$. Maximum selectivity for maleic anhydride on the oxidized phase is obtained at a lower oxygen partial pressure than on vanadyl pyrophosphate, which gives, however, the best overall selectivities. Furthermore, these authors have studied the non-steady-state catalytic behavior of these PVO catalysts and indicate that for both catalysts steady-state behavior is reached after about 5–10 h on stream. During transient behavior selectivity to maleic anhydride increases, but no clear indication of bulk/surface modifications is given.

Wenig and Schrader[41] claim that only (VO)$_2$P$_2$O$_7$ is the active and selective phase in n-butane oxidation to maleic anhydride. A slight "excess" of catalyst phosphorus (P:V = 1.1 catalyst) is necessary to stabilize the active phase. The excess phosphorus creates a distortion of the P$_2$O$_7$$^{4-}$ crystal environment. The α-VOPO$_4$ is considered by these authors as an active, but nonselective, phase. Shimoda et al.[52] also propose the vanadyl pyrophosphate as the active phase. They stress the importance of a stable well-defined crystalline structure. Amorphous V^{4+} phases or crystalline phases of V(V) (α- and β-VOPO$_4$) were found to be nonselective, and after use structural changes of the catalysts were not observed in the case of α- and β-VOPO$_4$ and (VO)$_2$P$_2$O$_7$. The results of Contractor et al.,[22] Johnson et al.,[91,111] Pepera et al.,[129] and Trifirò et al.[60,70,96,105,130] agree with the identification of vanadyl pyrophosphate as the active phase in n-butane oxidation. Contractor et al.[22] indicate that in the absence of gas-phase oxygen it is possible to eliminate highly active surface oxygen species that are not selective. Using a recirculating solids reactor, with separate hydrocarbon–catalyst and oxygen–catalyst stages, it is possible to increase the selectivity to maleic anhydride to near 80%.

Trifirò et al.[60,70,96,120,121,130-133] attribute only the activity of the catalyst to the V^{4+} phase (the vanadyl pyrophosphate), whereas the selectivity to maleic anhydride was connected to the presence of a very limited and controlled amount of V^V sites.[120,130-133] The selec-

tivity to maleic anhydride passes through a maximum[130] for a well-defined value of the degree of surface oxidation (number of V^{5+} ions with respect to the total amount of surface vanadium sites).

The same discordances as to the nature of the active phase are present in the literature concerning the optimal P:V atomic ratio of the catalysts, even though there is a general agreement that phosphorus stabilizes the +4 valence state of vanadium and limits its oxidation.[24,28,37,41,54,59,60,131] Van Geem and Nobel[34] studied catalysts with 0.3–2.4 P:V atomic ratio and concluded that the selectivity to maleic anhydride does not depend on the P:V ratio, but is only dependent on the degree of conversion of hydrocarbon. Garbassi et al.[37] have found that the specific conversion of n-butane increases by an order of magnitude for a P:V ratio just exceeding unity, but extended X-ray absorption measurements do not show any structural effect of the phosphorus.

The P:V ratio is a key parameter in determining catalyst selectivity and activity according to Wenig and Schrader.[41] Selectivity for maleic anhydride increases with catalyst phosphorus loading, whereas specific activity of both selective and nonselective oxidation decreases on increase of phosphorus content in the 0.9–1.2 P:V range. Best catalytic performances are exhibited with a catalyst with a P:V ratio of 1.1. Buchanan and Sundaresan[134] in an extensive kinetics study found that a catalyst with P:V ratio of 1.0 was approximately twice as active as a catalyst with P:V ratio of 1.1, while the selectivities to maleic anhydride were similar. Furthermore, they suggest that only surface P:V ratio is important because the transient kinetics results indicate the redox processes under reaction conditions are limited to a near-surface region, according to data of Pepera et al.[129]

However, the P:V surface atomic ratio of PVO catalysts as determined by X-ray photoelectron spectroscopy can be very different. Garbassi et al.[37] found a value of P:V surface ratio in the 2.0–2.8 range for P:V bulk ratios in the 1.0–1.4 range. Hodnett and Delmon[28,39] report that the surface P:V ratio is 1 for bulk stoichiometric P:V values of 1 or higher. They conclude[38–40] therefore that the reactivity of near-surface layers is hardly affected by the P:V ratio, but bulk reactivity is drastically curtailed.

Selectivity to maleic anhydride from n-butane maximizes for P:V = 1.0 according to Ai,[42] and they that associate this catalytic effect with the presence of strong-acid sites to activate n-butane. Finally, an optimal value of P:V around 1.0 was suggested by Contractor et al.[22] and by Trifirò et al.[60,70,105,131]

In conclusion, the scientific literature does not present a clear indication of the real nature of the active phase in n-butane selective conversion to maleic anhydride and the optimal characteristics for the PVO catalyst. This is partly related to the fact that sometimes only fragmentary and partial catalytic tests are presented from the authors, with poor information about the lifetime catalytic behavior of the examined catalysts. However, extensive analytical studies of used commercial vanadium phosphorus oxide catalysts from the fixed-bed butane process reveal the following:[135] (i) the equilibrated catalyst (after more than 200 h on stream), independent of the method of preparation (i.e., for example, in aqueous or organic solvent[96]), has an average P:V ratio of 1.00 $\mp$ 0.02; (ii) the oxidation state
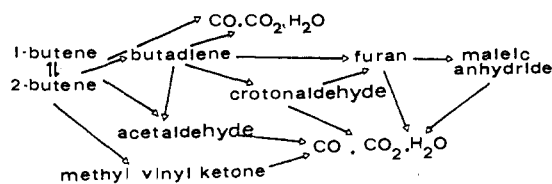

Figure 2. Possible reaction network[136] for the oxidation of but-1-ene on $(VO)_2P_2O_7$.
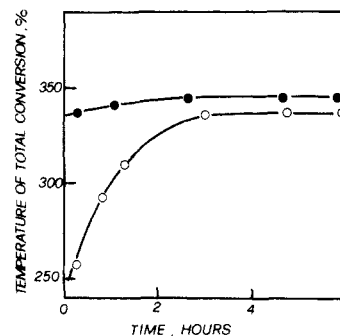

Figure 3. Temperature of hydrocarbon total conversion[69] as a function of time on stream on a high surface area fresh vanadyl pyrophosphate. Reactants: (O) but-1-ene; (●) n-butane.

of vanadium is 4.00–4.03; (iii) the X-ray diffraction pattern is attributed to a single crystalline phase, the vanadyl pyrophosphate.
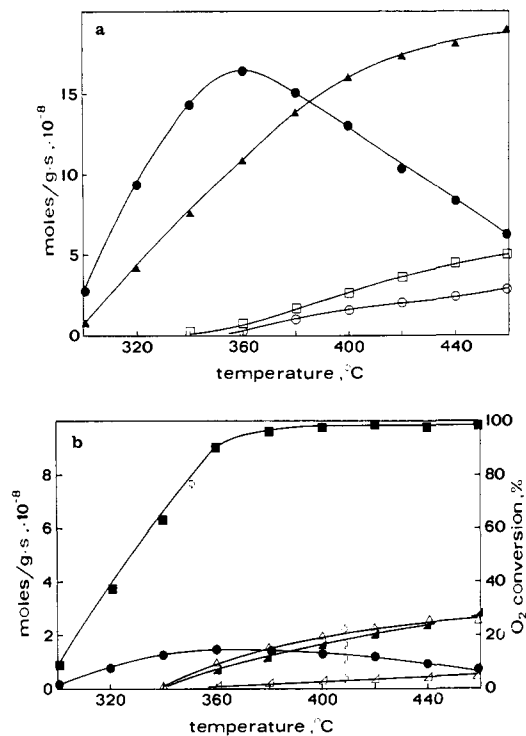
We may assume in the following discussion of the mechanism of n-butane conversion that these last results are really representative of the equilibrated active phase. Catalytic results for fresh catalysts (with time on stream less than equilibrated catalysts) will be assumed to be indicative of transient behavior and are useful to illustrate particular aspects of the mechanism of the reaction and the nature of active sites involved in the different steps.

III. Detection of Intermediates in the Oxidation of n-Butane under Steady-State and Transient Conditions

A. Steady-State Experiments

In the oxidation of C_4 olefins over vanadium phosphorus oxides, several products of partial oxidation are formed and detected,[136] as briefly outlined in the reaction network for the oxidation of but-1-ene in Figure 2. By comparison, only maleic anhydride, carbon oxides, and trace amounts of acetic acid and acrylic acid are detected in the oxidation of butane on the same catalyst[70] or on industrial catalysts.[7–19] Low yields of butenes and butadiene were detected by Moser and Schrader[113] on a $(VO)_2P_2O_7$ catalyst with very poor catalytic performance. These data on the mechanism may not be comparable with the more active catalysts for n-butane oxidation. The above observations suggest that the oxidation of n-butane may proceed without intermediate desorption from the active site instead of through a preliminary dehydrogenation step to butenes followed by a mechanism analogous to that for the formation of maleic anhydride from butenes.

To clarify this important question, it is worthwhile to consider the relatives rates of oxidation of butenes and n-butane on the same catalyst to determine

Figure 4. Effect of the temperature on the formation of products in n-butane oxidation at high paraffin concentration[133] on vanadyl pyrophosphate: (a) maleic anhydride (●), carbon oxides (▲), but-1-ene and but-2-ene (□), butadiene (O); (b) oxygen conversion (■), acetic acid (●), furan (△), crotonaldehyde (◢), methyl vinyl ketone (◿). Feed: oxygen concentration, 10%; n-butane concentration, 30.5%.
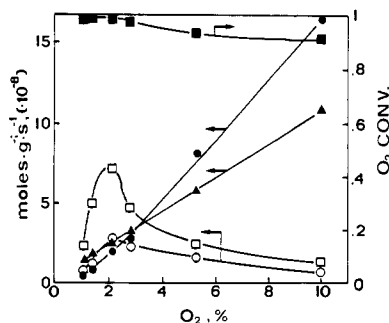
whether the nondetectability of intermediates is a consequence of differences in the kinetic constants for alkane versus alkene oxidation. However, at least on the PVO catalysts more active in n-butane oxidation, the interaction with the olefinic hydrocarbon leads to a rapid loss of surface area of the catalyst[69] and a rapid decrease of the activity (Figure 3). Thus, it is not possible to reliably compare the olefin and paraffin kinetic constants on the same PVO surface. However, a comparison of initial activities at non-steady-state conditions[133] suggests the ratio of the rate of butene oxidation to the rate of butane oxidation (assuming first-order kinetics for both reagents) is higher than 50. For consecutive first-order reactions of the type

$$n\text{-butane} \xrightarrow{1} \text{butenes} \xrightarrow{2} \text{maleic anhydride} \quad (3)$$

the maximum expected concentration of olefins is given by[137]

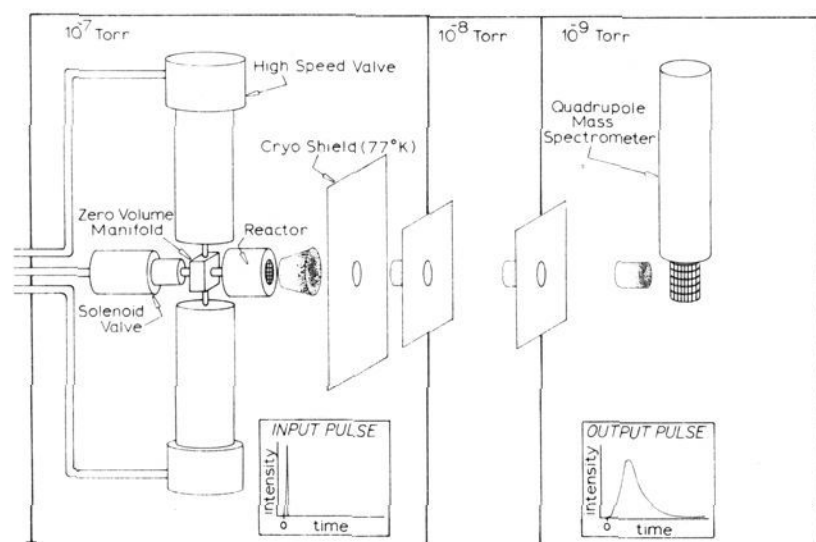$$\frac{C_{max,olefins}}{C_{0,butane}} = \frac{k_1^{k_2/(k_2-k_1)}}{k_2} \quad (4)$$

For an initial concentration of n-butane of 1%, the maximum concentration of intermediate olefins formed is very low, and therefore the nondetectability of olefins in the oxidation of n-butane in steady-state experiments could be justified for kinetic reasons. In order to increase the detectability of intermediates, two experimental approaches can be used. In accordance with eq 4, experiments at high n-butane concentrations (about 30%) favor the detection of intermediates. In addition, fast nonequilibrium transient experiments that are possible in a TAP (temporal analysis of products) re-

Figure 5. Effect of oxygen concentration on the formation of products in n-butane oxidation at high paraffin concentration[133] on vanadyl pyrophosphate: (■) oxygen conversion; (●) maleic anhydride; (▲) carbon oxides; (□) but-1-ene and but-2-ene; (O) butadiene. Note: to facilitate reading of the graph, the mol g^{-1} s^{-1} of butenes and butadiene are twice the actual values found. Feed: n-butane concentration, 30.5%; reaction temperature: 360 °C.

actor[71,72,138] make intermediate detection possible. Results from these two types of experimentation lead to similar conclusions.
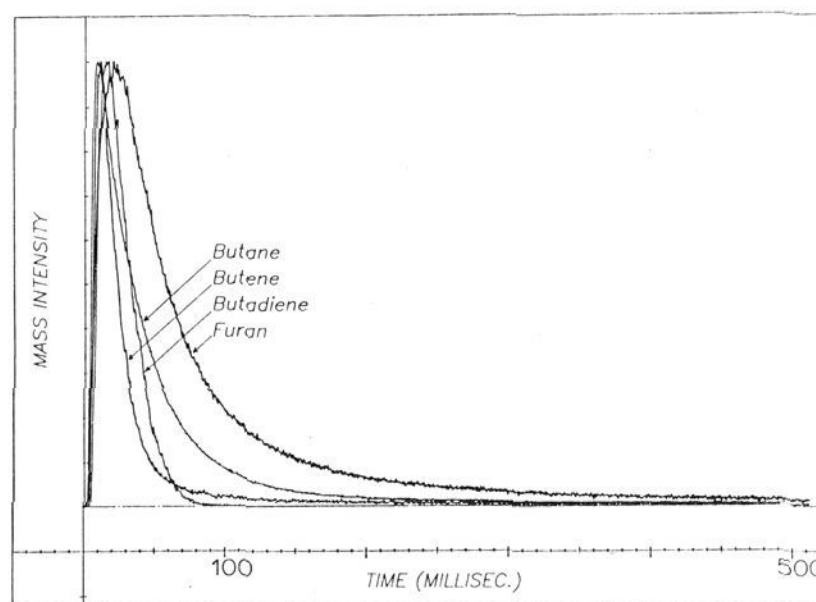
At high n-butane concentrations (about 30%), it is necessary to decrease the oxygen concentration to under approximately 10% in order to keep outside the explosion limits. Under these experimental conditions, the limiting reagent is the oxygen. Figures 4 and 5 report the results obtained[133] in the oxidation of n-butane at high concentration of hydrocarbon as a function of the reaction temperature and the oxygen concentration. In contrast to the results of catalytic tests at low hydrocarbon concentrations, high amounts of butenes, butadiene, and other byproducts similar to those seen in the direct oxidation of olefins are obtained. Similar byproducts are observed either by decreasing the oxygen concentration directly or by depleting the amount of available oxygen through chemical reaction at higher temperatures. It is worthy of note that the formation of typical products of butene and butadiene direct oxidation[59,139] such as methyl vinyl ketone or crotonaldehyde exactly coincides with the appearance of the former as products in n-butane oxidation (Figure 4). It might be argued that they form by consecutive interaction of the desorbed olefins with the catalyst surface. In all cases, the concentration of byproducts is greatest when the oxygen conversion is 100%. These results suggest the amount of oxygen present at the surface is an important factor in the formation of olefins and other byproducts. However, the very highly reducing conditions necessary in order to isolate the intermediates in steady-state conditions suggest these products may form on a significantly modified catalyst surface. Grasselli et al.[130,140] have shown that the "density of oxidizing sites" is a tool for modifying the selectivity in reactions of selective oxidation. With increase in degree of reduction of a metal oxide surface it is possible to control the nature of the product of oxidation. Products of partial oxidation may be obtained only through site isolation of the oxidizing centers. Similarly, the highly reducing conditions utilized (Figures 4 and 5) probably do not change the mechanism of reaction, but only the distribution of the active sites. A reduced degree of surface oxidation limits the rate of consecutive oxidation of the intermediates of reaction and allows their desorption into the gas phase.

Figure 6. Schematic diagram of the TAP (temporal analysis of products) reactor[71] system depicting the movement of a gas pulse from the microreactor to the QMS detector.

Figure 7. Single-pulse format data[71] presenting the normalized mass intensity vs time curves of desorbing reaction intermediates produced by pulsing a 4:1 O_2/butane mixture over $(VO)_2P_2O_7$ at 420 °C. The times of peak maximum are 8.2 ms (butane), 11.4 ms (butene), 16.5 ms (butadiene), and 22.5 ms (furan).

B. Time-Resolved Analysis

The TAP reactor is a unique, transient type catalyst evaluation system[71,72,138] that has been specifically designed for detection of reaction intermediates and determination of reaction sequences (Figure 6). Using high-speed injections (200-μs pulse widths) of molecular feed into a 0.5-mL reactor containing 500-μm catalyst particles, it is possible to identify and track the formation of intermediates as a function of time with millisecond time resolution. Since the reactor is embedded in a vacuum chamber and the analytical detection system is a quadrupole mass spectrometer separated from the reactor by differentially pumped chambers, desorbing intermediates have an essentially collision-free path to the detector. Moreover, a typical pulse intensity of 10^{15} molecules will address only about 10^{-4} of the total surface area of 1 g of a 10 m^2/g vanadium phosphorus oxide catalyst. This means the surface is not significantly perturbed by several thousand pulses of reactants. When a $(VO)_2P_2O_7$ catalyst equilibrated in a conventional fixed-bed reactor is examined in the TAP system with pulses of a 4:1 mixture of oxygen/butane at 420 °C and 1–2% butane conversion,[71] the entire series of intermediates in the butane oxidation reaction is observed (Figure 7). The product peaks are actually about 100 times less intense than the butane peak, but the peak maxima are normalized in the figure to facilitate time comparisons. The observed products are butene, butadiene, furan, carbon dioxide, and water. The carbon dioxide and water peaks are not displayed, and the carbon monoxide, which also is formed, cannot be deconvoluted from the other fragments at mass 28. In addition to showing the formation of intermediates at higher oxygen to hydrocarbon ratios, the reaction sequence is indicated. Comparison of the curve times of the intermediates to the butane curve shows that the individual peak maxima are shifted to later times relative to the butane maximum, following the order expected for stepwise butane oxidation. Note the butene curve decays more rapidly than the butadiene curve, which decays more rapidly than the butane curve. This is a result of the rapid conversion of the olefins to other products. In similar experiments using butene or butadiene as the initial reactant, conversions as high as 50% are observed. The lack of sharp decay in the case

of the furan curve indicates that very little furan is converted to products, and this is consistent with the fact that no maleic anhydride is observed. However, when the catalyst is first pulsed extensively with oxygen at reaction temperature and subsequently pulsed with a 4:1 oxygen/butane mixture, maleic anhydride is observed and the intermediate products are not. Continued pulsing with the reactant mixture eventually leads to the reappearance of intermediate products. These results indicate the intermediates desorb when the $(VO)_2P_2O_7$ is not fully oxidized. Further, while butene and butadiene are readily oxidized to furan, furan is not readily converted to maleic anhydride on a partially oxidized surface.

These two very different approaches to determination of intermediates in n-butane oxidation lead to the same conclusions. The vanadium phosphorus oxides are able to dehydrogenate the n-butane to olefins, and these olefins react further to form partial oxidation products. When insufficient oxygen is channeled to the active site, intermediate products may desorb and react at other sites. When surface oxygen concentrations are high, the evidence supports a single-site mechanism for selective conversion of n-butane to maleic anhydride; i.e., once n-butane is activated, it remains bound to the surface in various forms until desorption as maleic anhydride occurs.

IV. Kinetics of C_4 Hydrocarbon Oxidation

A. n-Butane

Several studies have been made in recent years to derive kinetic expressions to describe the reaction sequence for n-butane oxidation to maleic anhydride in steady-state conditions on vanadium phosphorus oxides.[70,131,134,141~144]

Escardino et al.[141] studied the reaction in a fluid bed reactor using a catalyst with P:V = 0.8. A triangular reaction network was proposed. At low hydrocarbon partial pressures the behavior of the n-butane oxidation reaction was predicted with three single pseudo-first-order reactions. Oxygen chemisorption was identified as the rate-determining step at large butane pressure,

SCHEME I. Kinetic Model Utilized by Lerou et al.[144] in a Study of n-Butane Selective Oxidation to Maleic Anhydride on a VPO Catalyst

REACTION NETWORK

BUTANE ⟶ r_1 ⟶ MALEIC ANHYDRIDE

r_2 r_4 r_3 r_5

CO CO_2

ADSORPTION MODEL

$r_1 = k_1 K_B p_B p_{O2} / N$

$r_2 = k_2 K_B p_B p_{O2} / N$

$r_3 = k_3 K_B p_B p_{O2} / N$

$r_4 = k_4 K_{MA} p_{MA} p_{O2} / N$

$r_5 = k_5 K_{MA} p_{MA} p_{O2} / N$

$N = 1 + K_B p_B + K_{MA} p_{MA} + K_{H2O} p_{H2O}$

and at typical n-butane concentrations, the rate of depletion was controlled by the reaction between butane in the gas phase and surface adsorbed oxygen.

Wohlfahrt and Hofmann[142] studied a catalyst with P:V = 1.06 and extended the range of hydrocarbon and oxygen concentrations investigated by Escardino et al.[141] and found that n-butane is oxidized according to a rate equation of the type
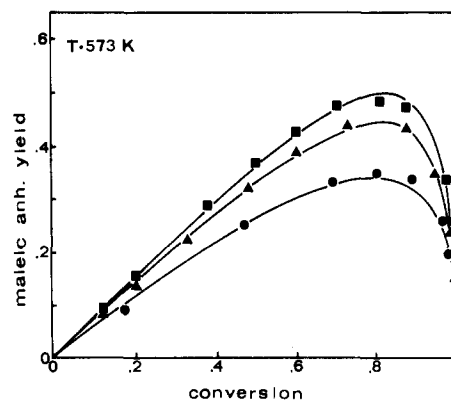
$$-r_B = \frac{k p_B p_O{}^{0.285}}{1 + K p_B} \tag{5}$$

and maleic anhydride is oxidized according to a rate equation of the type

$$r_{MA} = \frac{k p_{MA} p_O{}^{0.285}}{1 + K p_B} \tag{6}$$

where the subscripts B, O, and MA designate butane, oxygen, and maleic anhydride, respectively. However, the catalyst preparations adopted by these authors[141,142] for the kinetics analysis lead to catalysts with poor selectivity to maleic anhydride.

More recent kinetics studies[70,134,143,144] have been conducted on catalysts with higher selectivities and yields to maleic anhydride (50–60% molar yield). Substantial inhibition of the oxidation reaction by maleic anhydride and water was found by Sharma and Cresswell,[143] Lerou,[144] and Buchanan and Sundaresan.[134] The lattermost authors,[134] however, include the water and maleic anhydride effects in a single lumped term involving only the maleic anhydride concentration. The adsorption model proposed by Lerou[144] gives the best fit to experimental results, and it is based on the reaction model reported in Scheme 1.

Most of the kinetics studies found an order of reaction 1 for the dependence of the rate of n-butane depletion upon hydrocarbon partial pressure. However, these kinetics studies present some discordances. The more relevant are the reaction order for the dependence of the rates on oxygen partial pressure and the activation energies of the different rates. A low oxygen order dependence for the rate of n-butane depletion was found by Wohlfahrt and Hofmann[142] and by Centi et al.[70] (0.28 and 0.23, respectively), whereas the reaction order was 0.5 according to the Sharma model[143] and 1.0

Figure 8. Maleic anhydride yield at 300 °C conversion[70] on a high surface area fresh vanadyl pyrophosphate: (●) 0.32% n-butane; (▲) 0.70% n-butane; (■) 1.10% n-butane. O_2/n-butane = 15.0 in all tests.

according to adsorption model proposed by Lerou.[144] The Buchanan and Sundaresan[134] two-step redox kinetics model leads to a rate expression for butane oxidation of the form

$$r = k c_B / [1 + K_1 c_B / c_O{}^n + K_2 c_{MA} / c_O{}^n] \tag{7}$$

where the exponent n of the oxygen concentration can be 0.5 or 1.0 and not affect the fitting of the data. The redox model is based on transient experiments showing that PVO catalysts supply oxygen for the oxidation of butane even in the absence of O_2 in the feed mixture.[40,129,145] Activation energies are also different according to the various research groups, but it may be roughly correlated to the observed dependence on oxygen concentration. Lower activation energies were found by Wohlfahrt and Hofmann[142] and by Centi et al.,[70] whereas higher activation energies were reported by Buchanan and Sundaresan[134] and Lerou.[144] In light of these results and according to what was presented in the section on the structure of the catalyst, we will discuss the kinetics results and their relevance on the basis of the difference between catalytic behavior of fresh and equilibrated catalysts.

We refer to equilibrated catalysts as those in which the valence four of vanadium is well stable and its oxidation to V^{5+} is less dependent on the hydrocarbon/oxygen ratio in the reagent mixture. These catalysts show higher selectivities to maleic anhydride, especially at the higher conversions. These characteristics are representative of commercial catalysts equilibrated under the reaction conditions. The results of Buchanan and Sundaresan[134] and of Lerou[144] fit catalysts of this type. They show very little dependence of the catalytic behavior on a change of the hydrocarbon/oxygen ratio. Lerou[144] reports that the maleic anhydride yield decreases only for conversions higher than about 95%. For contact times higher than those corresponding to total conversion, the yield of maleic anhydride drastically decreases. Very comparable results are presented by Buchanan and Sundaresan.[134]

On the other hand, the kinetics results of Centi et al.[70] must be interpreted as indicative of the catalytic behavior of a fresh catalyst. A fresh catalyst possesses a higher rate of vanadium oxidation due to defects in the structure. The dependence of the maleic anhydride yield on the conversion (Figure 8) shows a well-defined maximum for a conversion of about 80%. A further
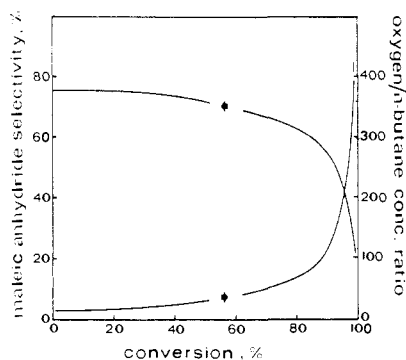
Figure 9. Selectivity in maleic anhydride and oxygen/n-butane residual concentration ratios as a function of the conversion.[70] Feed: 1.10% n-butane, O_2/butane = 15.0; reaction temperature: 300 °C; same catalyst as in Figure 8.

increase in conversion drastically decreases the yield of maleic anhydride to around 10% for total conversion. The decrease of selectivity to maleic anhydride parallels an increase of the ratio of residual concentration of oxygen to n-butane (Figure 9). This ratio is proportional to the oxidizing power of the reagent mixture, suggesting that at the end of the catalytic bed (corresponding to high conversion) the formed maleic anhydride is not stable in this catalytic system due to overoxidation of surface. An increase of V^V concentration at the end of catalytic bed was confirmed by chemical and spectroscopic analyses of the discharged catalysts.[69,131] In the kinetics models of Buchanan and Sundaresan[134] and Lerou[144] the selectivity to maleic anhydride does not depend on the initial n-butane/oxygen ratio, whereas according to Centi et al.[70] the selectivity to maleic anhydride increases on increasing this ratio. This is because on the catalytic system of Centi et al.[70] it is important to limit the overoxidation of the formed maleic anhydride due to the higher degree of surface oxidation. Furthermore, this catalyst is more active and operates in a range of reaction temperatures about 100 °C lower than any previously examined catalytic system,[134,144] and thus the activation energy for n-butane depletion is lower.

We offer the following interpretation of the differences in the kinetic behaviors in n-butane oxidation observed by the different groups. In the catalytic system utilized by Centi et al.[70] the rate of oxidation of V^{4+} to V^{5+} is higher than in the other catalysts.[134,144] Therefore, in this system the dependence of the rate of n-butane depletion shows a reduced order in oxygen partial pressures. Also under these conditions the degree of surface oxidation is much more dependent upon reagent composition as well as on its change as a function of the conversion in the reactor bed. On the other hand, under these conditions the catalyst is more active and the rate of n-butane depletion has a lower activation energy due to enhanced redox properties of vanadium connected to the defective structure of the vanadyl pyrophosphate utilized. This is confirmed by the transient kinetics tests reported by Buchanan and Sundaresan.[134] The transient experiments were conducted in a flow reactor and the rate of n-butane depletion was determined after a rapid switching of the inlet feed mixture from a butane/air mixture with a high O_2/hydrocarbon ratio to a second feed mixture with a lower O_2/butane concentration ratio. The ob-

served rate of butane depletion was higher than expected for a period of about 1–2 min after the change, confirming the higher activity of an oxidized surface.

In the case of the catalytic systems utilized by Buchanan and Sundaresan[134] and Lerou[144] the lower rate of vanadium surface oxidation results in the observed higher reaction order in oxygen concentration and the reduced reactivity of the surface in the rate of both n-butane depletion and maleic anhydride consecutive oxidation.

In conclusion, the comparison of these kinetics results stresses the importance of surface catalyst redox level in determining the catalytic behavior (selectivity to maleic anhydride) as well as the role of the redox properties of vanadium (evidenced by the different activation energies) in determining the activity of the catalyst. From a mechanistic point of view, kinetics results of almost all authors indicate that the activation of n-butane is the rate-determining step, whereas some discordances are present in the literature concerning the activation of oxygen in the rate-determining step.

B. Butenes and Butadiene

As discussed in the previous section, the butenes and butadiene are intermediates in the mechanism of n-butane conversion to maleic anhydride, or, more exactly, the catalyst forms intermediates that may desorb as these olefins. Furthermore, since the first step of n-butane activation is the rate-determining step of the reaction, information on the reactivity and kinetics of the consecutive steps in steady-state can only be obtained by studying the kinetics of the intermediate olefins. In this section, we compare and comment on particular aspects of the kinetic behavior of these olefinic hydrocarbons. The kinetics of the 1- and 2-butenes and butadiene have been more extensively studied[43–46,139,146–151] than the kinetics of n-butane, but in this section we present only data useful for the mechanistic analysis of n-butane oxidation.

In the C_4 alkene oxidation an interesting effect is observed.[139,146,148] On increasing the hydrocarbon concentration, the formation of maleic anhydride reaches a maximum and then decreases with a corresponding increase in the formation of butadiene. An increase in oxygen partial pressure while keeping butene constant causes an increase in the formation of maleic anhydride. The olefin concentration corresponding to the value of the maximum maleic anhydride shifts to higher values on increase of oxygen concentration. Similar results are found in butadiene oxidation. Also a self-inhibition effect of the hydrocarbon on the synthesis of the maleic anhydride and an almost linear dependence of the self-inhibition effect upon the O_2 concentration are observed.

These data can be interpreted on the basis of a kinetic model[148] derived from the Langmuir–Hinshelwood mechanism in which the rate-determining step for maleic anhydride formation is surface reaction between adsorbed oxygen on a single site and the intermediate butadiene adsorbed on two adjacent sites. From a mechanistic point of view, these data lead to some interesting conclusions:

(i) The equivalence between deactivation of the sites for the synthesis of maleic anhydride and increase in the formation of butadiene is a further indication of the
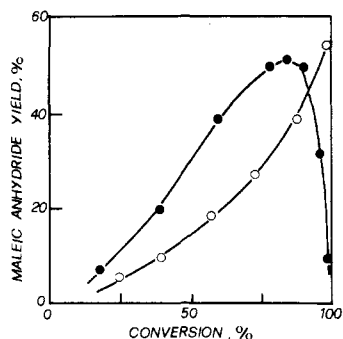
Figure 10. Dependence of the maleic anhydride yield on the conversion[69] in the oxidation of n-butane (●) and of but-1-ene (O) on a high surface area fresh vanadyl pyrophosphate.
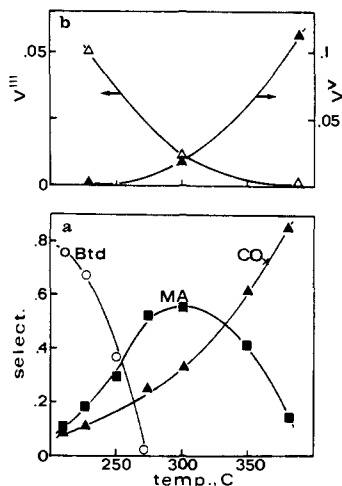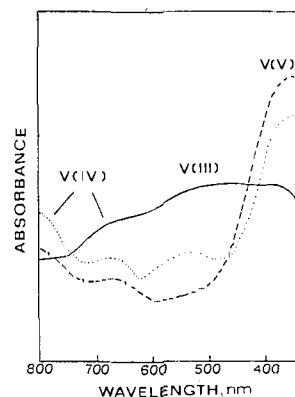

Figure 11. Effect of the reaction temperature on the selectivity of main products in but-1-ene oxidation[136] (a) and on the valence state of vanadium (b) for a vanadyl pyrophosphate catalyst (P:V = 1.01). Legend: (Btd) butadiene, (MA) maleic anhydride, (CO_x) carbon oxides. Feed: 0.6% but-1-ene, 12% O_2.

Figure 12. Diffuse reflectance spectra of the same catalyst as in Figure 11 after interaction with but-1-ene/air at different temperatures:[136] (—) 220 °C; (...) 300 °C; (- - -) 370 °C.

intermediate formation of butadiene (an adsorbed precursor of butadiene) in the mechanism from butenes to maleic anhydride.

(ii) The C_4 olefins strongly adsorb on the surface of the catalyst, and their adsorption inhibits that of the oxygen.

(iii) The rate-determining step in the conversion of butenes is not the hydrocarbon activation, but the surface step of oxygen insertion on the adsorbed activated hydrocarbon (that may desorb as butadiene in the absence of sites of oxygen insertion). The kinetic behavior is very different from the other known reactions of olefin selective oxidation, such as propene conversion to acrolein,[66,67] where the rate-determining step is the olefin activation by abstraction of an allylic hydrogen atom. In the oxidation of olefins on PVO catalysts, the most critical problem is maintaining the vanadium phosphorus catalyst at a sufficient degree of surface oxidation to allow the oxidation of the intermediate adsorbed hydrocarbon up to maleic anhydride. The very strong adsorption of these hydrocarbons on the surface of the catalyst inhibits the oxygen adsorption, thus maintaining the surface of the catalyst in a lower oxidation state. This also explains why some authors[50,59,152] indicate that the active phase in maleic anhydride formation from butenes is a mixture of vanadyl pyrophosphate (vanadium(IV)) and VOPO₄ (vanadium(V)).

Finally, it is worthwhile to illustrate the different trends of the yield of maleic anhydride vs hydrocarbon conversion found by Cavani et al.[69] in the oxidation of n-butane and butenes under similar conditions and on the same catalyst (Figure 10). Apart from the loss of selectivity at conversions higher than 80%, which depends on the specific nature of the catalyst, n-butane oxidation to maleic anhydride is more selective than the butene reaction. The reduced surface concentration of intermediates in the n-butane reaction (i) avoids their desorption (for example, butadiene is a typical product of but-1-ene oxidation at conversions lower than 100%) and (ii) makes possible their fast further transformation to useful product. This reaction of oxidation and oxygen insertion is inhibited by a high surface concentration of intermediates, as shown by the butene kinetic data. Both factors limit the possible parallel reaction of these intermediates, increasing the selectivity to useful product, maleic anhydride.

V. Surface Modifications by Interaction of C₄ Hydrocarbons with the Catalyst Surface

The very different kinetic behaviors of the alkene and alkane reactants bring into question the different catalyst surface effects induced by the two reactants.

Szakacs et al.[127] studied the oxidation of but-1-ene and n-butane to maleic anhydride in a pulse microreactor in the presence of gaseous O_2 on a VOPO₄ catalyst. Oxygen balances show that in both cases, in spite of the presence of gas-phase O_2, the V^V phosphate acts as the oxygen source. However, in the but-1-ene conversion the amount of lattice oxygen incorporated in the products of reaction is much higher than in the n-butane case, pointing out the substantial difference in the reactivity and of the type of interaction of the two hydrocarbons. Catalytic behavior in the pulse tests changed with the number of pulses, parallel to the modification of the catalyst surface.[127,136,153] This illustrates the relationship between surface modifications derived from the redox interactions of the hydrocarbon and oxygen with the catalyst surface and self-induced modifications on catalytic behavior. The working state of catalyst under steady-state conditions depends upon the nature of this dynamic interaction.[64,120,130] However, this also offers the possibility of studying the mechanism of reaction under steady-state dynamic conditions and analyzing the nature of the products formed as a
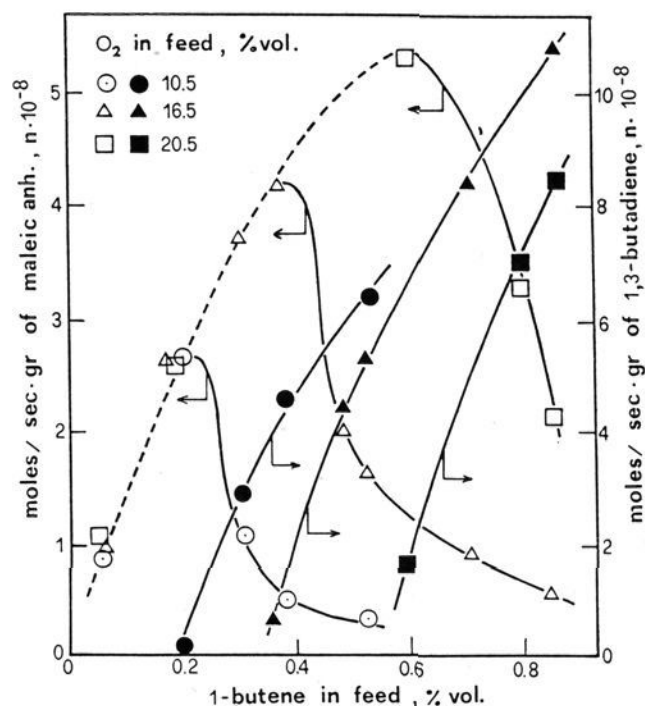
Figure 13. The formed mol g^{-1} s^{-1} of maleic anhydride (open symbols) and of butadiene (full symbols) in the oxidation of but-1-ene at different oxygen concentrations.[139] Reaction temperature: 405 °C.
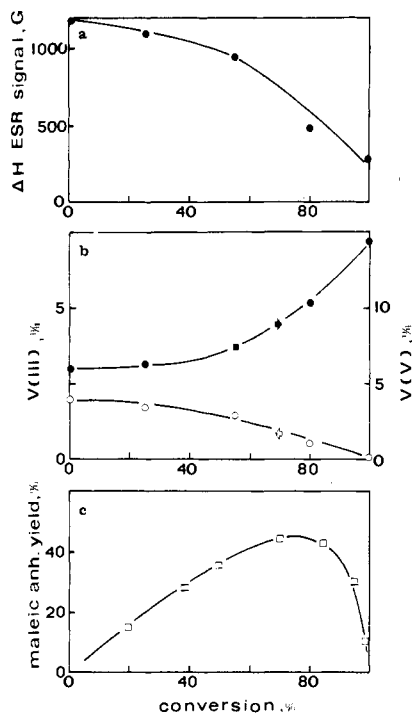

Figure 14. Valence state of vanadium after reaction tests in different conditions (a) and rate and selectivity of maleic anhydride formation in butane oxidation at 300 °C and 10% O_2 and different butane concentrations (b).[133]

function of the type of surface modifications induced by the hydrocarbon/O_2 interaction. Due to the higher reducing power and reactivity of butenes as compared to n-butanes, results with the former hydrocarbon will be compared with those of the alkane in order to highlight some aspects and the common features of the mechanism of reaction.

Figure 11 illustrates the main products obtained in but-1-ene oxidation as a function of increasing reaction temperature and the relative amount of V^{III} and V^V present in the catalyst (the balance is present as V^{IV}).[136] X-ray diffraction in all cases shows only the presence of the $(VO)_2P_2O_7$ phase. Three ranges of catalytic behavior can be distinguished: (i) at lower temperatures, the main product is butadiene; (ii) at an intermediate temperature, the main product is maleic anhydride; and (iii) at the higher temperature, carbon oxide formation predominates. The catalysts that are 100% V^{IV} before the catalytic tests are reduced at low temperatures and oxidized at high temperatures.[120,136] The reaction of the but-1-ene/oxygen mixture strongly affects the nature of the catalyst as a function of the reaction temperature. Variations of the oxidation state of the catalyst under the aforementioned three conditions are also shown by the diffuse reflectance spectra[136] in the UV–vis region (Figure 12). Results from the surface interaction with the hydrocarbon/oxygen mixture carried out as a function of the relative concentration of hydrocarbon and oxygen parallel those obtained[69,120,136] by varying the reaction temperature at a fixed concentration. An increase of the but-1-ene/oxygen ratio results[139] in a decrease of the rate of maleic anhydride formation and an increase of the rate of butadiene formation (Figure 13) with a corresponding disappearance of V^V and reduction to produce V^{III}. An increase in the oxygen concentration results in an increase in the amount of V^V and of the rate of maleic anhydride formation.

The good agreement between catalytic behavior (main product formed in the oxidation of but-1-ene in steady-state conditions) and surface-induced modifications[120,136] suggests that the two different steps of oxidative dehydrogenation from but-1-ene to butadiene
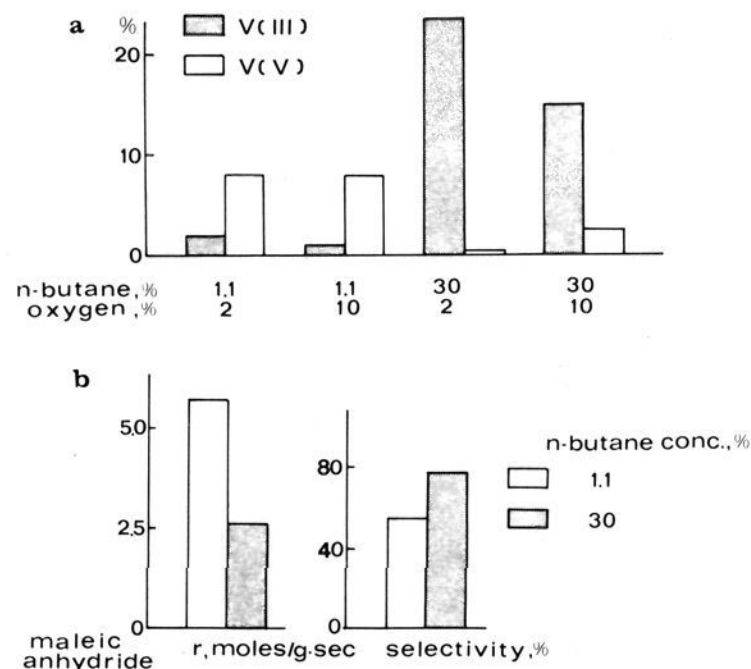
and oxidation from butadiene up to maleic anhydride require different valence states of vanadium. V^{IV} reduction to V^{III} is required for the first step, and V^V reduction is required for the second step.

When n-butane is oxidized under the same conditions, the degree of catalyst reduction is less than that observed with but-1-ene.[69] The catalyst exhibits less deactivation with the alkane compared with the alkene (Figure 3). However, when increased n-butane/oxygen ratios are used to observe the formation of intermediate olefin from n-butane[133] (Figures 4 and 5), a deeper reduction of the catalyst is seen as reflected by the formation of high amounts of V^{III} (Figure 14a.)[133] Under these conditions, as in the case of but-1-ene, the vanadyl pyrophosphate catalyst rapidly and irreversibly deactivates,[133] but becomes more selective (Figure 14b).

On the fresh catalyst used by Centi et al.[70] for their kinetics study, a critical factor governing the selectivity at very high butane conversions is the instability of the formed maleic anhydride in the back end of the catalytic bed. It is thus worthwhile to analyze the variations in the catalyst surface as a function of position in the catalytic bed.[120,131] Figure 15 reports the valence state of vanadium (determined by chemical analysis), the broadness of the EPR signal of VO^{2+} ions in the catalyst (the broadness is associated with and proportional to the concentration of V^{III} in the sample), and the yield of maleic anhydride as a function of the conversion. Figure 8 illustrates the variation of the oxygen/hydrocarbon ratio as a function of the conversion. These results suggest that enhanced formation of V^V at the end of the catalyst bed is directly attributable to the more oxidizing atmosphere present. This increased concentration of V^V substantially decreases the final yield of maleic anhydride, most probably due to an enhanced rate of maleic anhydride decomposition on the fresh catalyst used by these authors.[120,131] On equilibrated catalysts, this effect is much less evident, due to the reduced rate of vanadium oxidation to V^V. This factor is important only for contact times higher than those required to achieve 100% conversion[144] (presence of only residual O_2 in the flow) or for very high oxygen/n-butane ratios.[134] The recent results of

Figure 15. (a) Broadness (ΔH) of the EPR signal of VO^{2+}, (b) valence state of vanadium determined by chemical analyses, and (c) maleic anhydride yield as a function of the hydrocarbon conversion at 300 °C on a high surface area fresh vanadyl pyrophosphate.[131] Feed: 0.7% n-butane, oxygen/butane = 15.

Miyamoto et al.[154] on the oxidation of n-butane on various unsupported or supported V^V oxides confirm that V^V=O species are very active in total combustion of butane.

These experimental results illustrate the important relationship between catalytic behavior and the surface modifications induced by the medium itself. The redox properties of the feed influence the surface oxidation state of the catalyst, which in turn profoundly affects the nature of the products formed in the reaction. In the oxidation of both n-butane and but-1-ene, partial oxidation products (butadiene in but-1-ene oxidation, or butenes and butadiene in n-butane oxidation) are observed at low oxygen concentrations when a very limited number of vanadium(V) species are present on the surface of the catalyst or when nonequilibrium conditions at reduced pressures are employed as in the TAP experiments.

The change of valence state of vanadium thus depends upon a balance of three factors: (1) the redox potential of the feed, (2) the rate of oxidation of the catalyst at the temperature of reaction, and (3) the rate of reduction of the catalyst at the temperature of reaction. Literature results are in line with these conclusions. However, a deeper examination of the dynamics of the working state of the catalyst surface and the relationship between surface-induced modifications and catalytic behavior would lead to an even better understanding of the selectivity-controlling properties of these mixed oxides.[130]

VI. Relationship between Redox Properties and Catalytic Behavior

As pointed out in the section on catalyst structure, the binary vanadium phosphorus oxide system is rather
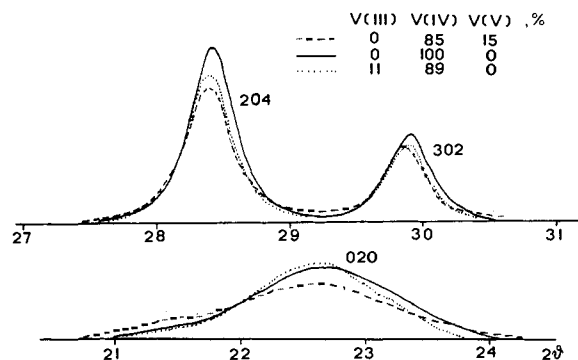
Figure 16. Effect of the presence of different valence states of vanadium on the principal X-ray diffraction lines of vanadyl pyrophosphate (P:V = 1.0).[136]
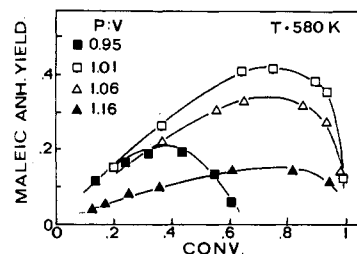
Figure 17. Maleic anhydride yield vs conversion of n-butane for high surface area fresh VPO catalysts with different P:V atomic ratios.[131] Feed: 0.7% n-butane, 12% O_2.
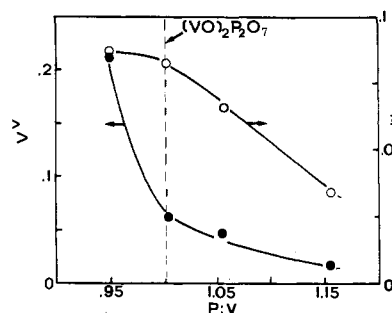
Figure 18. Effect of the P:V atomic ratio[136] on the percent of V^V and of V^{III} formed after 0.5 h at 400 °C in a flow of air (oxidation) and after 0.5 h at 500 °C in a flow of 2% H_2/He (reduction). Initial catalyst: high surface area fresh $(VO)_2P_2O_7$, 100% V^{IV}.

complicated because of the great variety of observed phases and the difficulties encountered in the development of successful and reproducible syntheses of pure single phases stable under reaction conditions. Over the past few years improved understanding of the factors determining the structure of PVO has allowed the development of suitable methods of preparation of vanadyl pyrophosphate. In particular, the preparation of vanadyl pyrophosphate active phase in organic media, i.e., utilizing an organic alcohol as solvent and also as the reducing agent for the V^V starting compound,[60] not only results in more active catalysts for n-butane oxidation[26,60,70] but allows preparation of compounds with 0.95–1.2 P:V atomic ratio and variable mean valence states of vanadium (up to about 20% of V^V) without significant changes of X-ray diffraction patterns (Figure 16) and cell parameters.[136]

It is thus possible to modify and study the P:V ratio around the stoichiometric value (P:V = 1.0) without the formation of other crystalline phases. As illustrated in Figures 17 and 18, the variation of the content of P in

the composition modifies the catalytic properties in n-butane oxidation[131] and butene oxidation[60] (Figure 17) and the redox properties of the catalysts,[136] i.e., the rate of V^{IV} oxidation to V^V and the rate of V^{IV} reduction to V^{III} (Figure 18). With respect to the stoichiometric ratio of the $(VO)_2P_2O_7$, a slight deficiency of phosphorus does not change the rate of V^{IV} oxidation to V^V. On the other hand, an excess of phosphorus only slightly influences the rate of oxidation, but strongly affects the rate of reduction. This effect is in part attributed to a decrease of the number of the active sites, but also reflects a particular kind of interaction of phosphorus upon the vanadium ions, as shown by the trend of activation energies of reduction and oxidation with respect to the P:V ratio.[106,136] Similar results are obtained by studying the amount of V^{III} formed in the catalyst by interaction with a mixture of but-1-ene/oxygen as a function of time of reaction and of P:V atomic ratio in the catalyst.[136] In order to correlate the observed variations in the redox properties with the catalytic behavior in n-butane oxidation on the fresh catalyst used by these authors,[136] it is necessary to distinguish between tests at low conversion (lower than 10%) where the reducing power of the reagent mixture is higher and catalytic tests at high conversion (Figure 17). At low conversion, the catalysts with P:V ratio 0.95 and 1.01 show the same activity, selectivity, and kinetic behavior.[131] However, at high conversion of n-butane (80%) the catalyst deficient in phosphorus and with the observed higher rate of vanadium oxidation forms primarily carbon oxides. The catalysts with more phosphorus with respect to the stoichiometric ratio of 1.0 are less active (Figure 17) and less selective already at low conversion,[131] but do not show the strong decline of maleic anhydride selectivity at the highest conversions. For these vanadyl pyrophosphate catalysts,[131,136] a content of phosphorus lower than required for stoichiometric P:V = 1.0 principally influences the rate of consecutive oxidation of maleic anhydride, whereas for catalysts with a higher amount of P with respect to P:V = 1.0, the predominant effect is on the rate of formation of maleic anhydride. It is reasonable to correlate these catalytic effects with the redox properties of the catalyst.[136] The strong increase of the rate of vanadium oxidation in the phosphorus-deficient catalyst leads to an enhancement of the rate of consecutive oxidation of maleic anhydride (effect on the selectivity), whereas the decreased rate of reduction of vanadium in the catalyst with higher P content than a stoichiometric one leads to the reduced rate of hydrocarbon depletion (effect on the activity).

Zein El Deen and Baerns[153] noted a similar effect. When PVO catalysts were treated in a cyclic fashion with pure O_2 followed by butenes, the selectivity in maleic anhydride formation diminished as compared with steady-state behavior. Nakamura et al.[47] also suggested that some V^{5+} ions were necessary for maleic anhydride synthesis, but the optimum mean valence state of catalyst is close to four. Similar conclusions were presented recently by Wenig and Schrader[41] studying the effect of phosphorus on the kinetic behavior of PVO catalysts in n-butane oxidation. They report catalyst phosphorus loading is a key parameter in determining catalyst selectivity and activity. An increase of P content in the 0.9–1.2 P:V atomic ratio decreases specific activity in n-butane depletion and
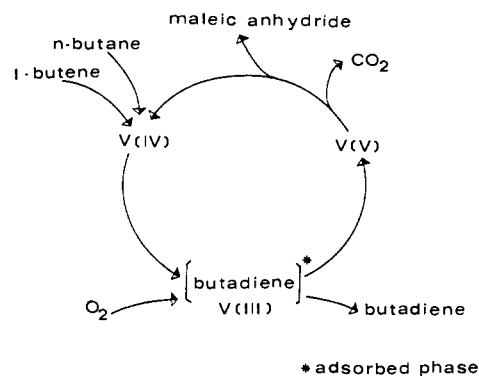
Figure 19. General scheme for C_4 hydrocarbon oxidation on VPO catalysts.[107]
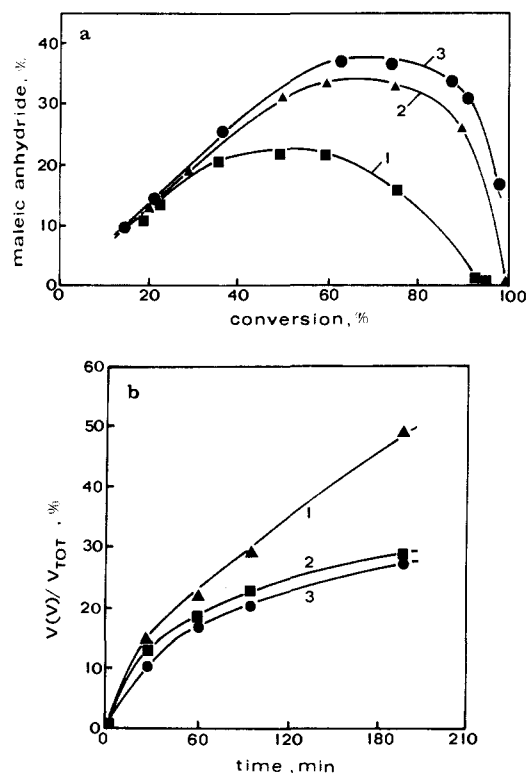
Figure 20. (a) Maleic anhydride yields vs conversion at 300 °C in n-butane oxidation[96] for different catalysts with P:V = 1.0. Feed: 0.6% n-butane, 12% O_2. (b) Rate of V^{IV} oxidation to V^V (in air at 400 °C) for the same catalysts of (a).[96]

increases the selectivity to maleic anhydride. However, these catalysts show an unusual low activation energy; approximately 100 °C is necessary in order to double the rate of n-butane depletion. The same selectivity, on the contrary, was reported by Buchanan and Sundaresan[134] in their kinetic study on two PVO catalysts with P:V = 1.0 and 1.1, respectively. The former catalyst was approximately twice as active as the P:V = 1.1 catalyst. Pyatnitskaya et al.[35] also found a correlation in vanadium phosphorus oxides between the concentration of V^{4+} ions in the discharged catalysts and the activity in n-butane oxidation. It is worth noting that they also noted the presence of V^{3+} ions in the catalysts. Nakamura et al.[47] also deduced the presence of V^{3+} ions in the discharged catalysts after the catalytic experiments on the basis of the broadening of the vanadyl EPR signal.

Figure 19 summarizes the relationship between redox properties of vanadyl pyrophosphate and catalytic be-

havior in C_4 hydrocarbon oxidation. The results of surface modifications induced by the interaction of C_4 hydrocarbons as well as the results of P:V ratio effect on redox properties and on selectivity/activity are interpreted on the basis of two different types of reaction in going from the alkane or alkene to maleic anhydride: a first step of oxidative dehydrogenation up to adsorbed butadiene and a second step of further oxidation of this intermediate. The first step is suggested to be controlled by the rate of V^{IV} reduction, whereas the second step is controlled by the amount of V^V available. However, when the content of V^V is too high, the oxidation proceeds further to carbon oxides.

These data suggest a strong relationship between selectivity to maleic anhydride at high conversion and rate of formation of vanadium(V). This is illustrated for catalysts with the same P:V ratio in Figure 20, which shows the rates of V^V formation (Figure 20b) and the corresponding maleic anhydride yields vs butane conversion (Figure 20a).[96] The different redox properties of the three catalysts (only crystalline phase, the vanadyl pyrophosphate) depend upon the preparation procedures.[96] At low conversion and similar rates of V^V formation the catalysts show approximately similar selectivity, but at high conversion, when the greatest disparity in rates of oxidation exists, the more oxidizable catalyst shows the highest rate of maleic anhydride decomposition.

VII. Mechanism of n-Butane Activation

Kinetics data agree that the hydrocarbon activation is the first step in n-butane oxidation.[70,134,141-144] The question to be addressed is whether this activation and breaking of a C–H bond occurs by real charge separation (H⁺ and RCH_2^- or H⁻ and RCH_2^+) or occurs without charge separation. Kung[65] discussed this concept on the basis of the heats of reaction ($\Delta H°$) of the C–H bond dissociation process with and without charge separation. In the gas phase, due to the energy required for charge separation, the heterolytic process is unfavorable. The catalytic process, however, would require less energy because the hydrogen atom or proton would form O–H bonds with the surface oxygen and the hydrocarbon intermediate is stabilized by surface interaction. However, Kung[65] suggests that since the alkane is rather inert, the transition state of the activation step is reactant-like and the activation energy in an alkane series would parallel $\Delta H°$ values of the gas-phase process. Kung[65] concluded that for saturated hydrocarbons the rate-determining step is the dissociation of the C–H bond in a manner similar to the production of hydrocarbon free radicals. Furthermore, he suggests that the step of C–H bond breaking in the alkane is thermodynamically favorable if the energy of oxygen–lattice interaction lost when the O–H bond is formed is weak. This would require a very reactive oxygen that is bound weakly to the solid for it to be thermodynamically favorable. It is known from the literature that O⁻ and O_2^- species (one oxygen molecule may be activated by accepting electrons from the solid or alternatively, O⁻ species may form by decomposition of N_2O) are very reactive in the oxidative dehydrogenation and activation of light alkanes.[155-160] In summary, highly reactive surface oxygen (weakly adsorbed oxygen and/or

localized surface lattice defects) is the active site for alkane activation according to Kung.[65] Matsuura[152] and Szakacs et al.[127] also suggested O⁻ species as the active sites for abstraction of hydrogens from butane. According to the latter authors,[127] these species do not form by direct oxygen interaction, but with the following mechanism:

$$V^{5+} + O^{2-} \overset{\Delta}{\rightleftharpoons} V^{4+} + O^- \qquad (8)$$
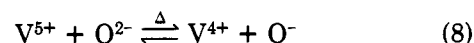
Activated oxygen species (O*) were indicated also by Ebner et al.[71,161] to be responsible for the butane activation step. Oxygen chemisorption experiments suggest that much of the surface vanadium in $(VO)_2P_2O_7$ is available for oxygen chemisorption. Around 1 oxygen molecule was adsorbed per 3 surface vanadiums. The adsorption was largely irreversible, which implies a strong bond to the surface vanadium. They suggest that the oxygen chemisorption occurs via a dissociative pathway on vanadium dimers, leading to a V^{5+}–O* type surface species capable of activating the alkane. Multipulse TAP experiments[161] furthermore show that when the adsorbed oxygen species (designated O*) was removed on the $(VO)_2P_2O_7$ surface by the reaction of furan to maleic anhydride, the catalyst was no longer able to activate butane.

Weakly adsorbed and activated oxygen species are strongly electrophilic reactants, and their presence (determined, for example, by in situ work function measurements) was generally associated in the literature with total oxidation.[63,162] Furthermore, the higher selectivities in the absence of gas-phase oxygen obtained in n-butane conversion in a transport bed reactor[22] (separate stages of catalyst interaction with hydrocarbon and oxygen) are explained on the basis of the absence in these conditions of surface-active species like O_2^- and O⁻.

A second problem raised from the hypothesis of weakly adsorbed species as the active sites in butane dehydrogenation is the great selectivity of this reaction. Pepera et al.[129] studied the n-butane conversion to maleic anhydride on $(VO)_2P_2O_7$ using labeled compounds. Several interesting observations regarding the mechanism of n-butane activation are derived from this study: (i) The butane does not reversibly chemisorb with hydrogen exchange onto the surface of the vanadyl pyrophosphate during the oxidation reaction, but is only irreversibly adsorbed onto the surface. On the contrary, a reversible maleic anhydride adsorption does occur. (ii) The oxygen-equilibrated catalyst does not undergo exchange reactions with the gas phase, indicating the irreversibility of the surface reoxidation step. (iii) Isotope effects observed in deuteriated butane studies strongly indicate that butane conversion both to maleic anhydride and to combustion products goes through the same rate-determining step. Selectivity is determined during the fast steps after the initial C–H bond activation. (iv) The rate-determining step for the reaction of butane is the activation of a methylene carbon–hydrogen bond. The magnitude of this isotope effect observed indicates nearly exclusive reaction with this path. Less than 5% of the butane reaction proceeds by methyl C–H activation.

The highly reactive adsorbed and activated oxygen species proposed as active sites for the reaction (for example, O⁻) would be expected to show selectivity for
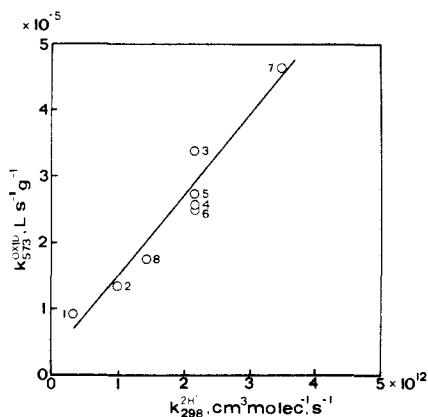
Figure 21. Correlation[165] between the rate constant of alkane depletion (K^{ox}) at 573 K (first-order rate equation) and the rate constant (K^{2H}) at 298 K for the hypothetical reaction of simultaneous 2 H abstraction from the alkane (calculated as a function of the nature of R_1, R_2, R_3, and R_4 on the basis of the data and equations reported by Atkinson[166]) according to reaction 13. Legend: (1) ethane, (2) propane, (3) n-butane, (4) n-pentane, (5) n-hexane, (6) n-heptane, (7) 2-methylbutane, and (8) cyclohexane.

$$\begin{matrix} R_1 \\ \diagdown \\ CH-CH \\ \diagup \\ R_2 \end{matrix} \begin{matrix} R_3 \\ \diagup \\ \\ \diagdown \\ R_4 \end{matrix} \xrightarrow[\text{contempor}]{2OH^-} \begin{matrix} R_1 \\ \diagdown \\ C = C \\ \diagup \\ R_2 \end{matrix} \begin{matrix} R_3 \\ \diagup \\ \\ \diagdown \\ R_4 \end{matrix} \qquad (13)$$
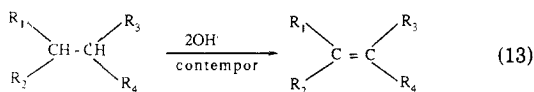
the C–H bonds only in a statistical sense.[160] V(IV) may be, on the contrary, simply viewed as a transition-metal radical. With its d orbital based unpaired electron being much less reactive, it would be expected to discriminate between the methylene and stronger methyl C–H bonds. Pepera et al.,[129] therefore, conclude that V(IV) at the surface of vanadyl pyrophosphate may be the key to selective activation, acting in the homolytic cleavage of the methylene C–H bond of butane.

Recent results by Centi and Trifirò[105,163-165] suggest a different hypothesis for the activation of butane. The energies for homolytic and heterolytic breaking of C–H bonds are different according to the specific nature of the alkane. For example, the probability of homolytic bond dissociation follows the order

$$\text{tertiary C–H} > \text{secondary C–H} > \text{primary C–H} \qquad (9)$$

Furthermore, if the rate-determining step is not only the abstraction of one hydrogen atom, but the contemporaneous abstraction of two hydrogen atoms, further differences in the reactivities of alkane are expected. Centi and Trifirò[165] have compared the reactivity of the C_2–C_7 alkane series on vanadyl pyrophosphate, trying to correlate the observed kinetic constants of hydrocarbon depletion with the kinetic constants derived from literature data[166] for the theoretical reaction of (i) simultaneous abstraction of two hydrogen atom radicals or (ii) the abstraction of only the first hydrogen. Figure 21 shows the results[165] obtained. Fitting of the data of reactivity is possible only on the basis of the hypothesis that the rate-determining step is the contemporaneous removal of both of the two methylene hydrogens from the carbon atoms in the 2- and 3-positions of the n-butane molecule.

However, the rate of n-butane depletion is structure sensitive[26] and sensibly depends upon the method of preparation of vanadyl pyrophosphate. The specific centers for the selective activation of the alkane are present in a very different amount depending on the
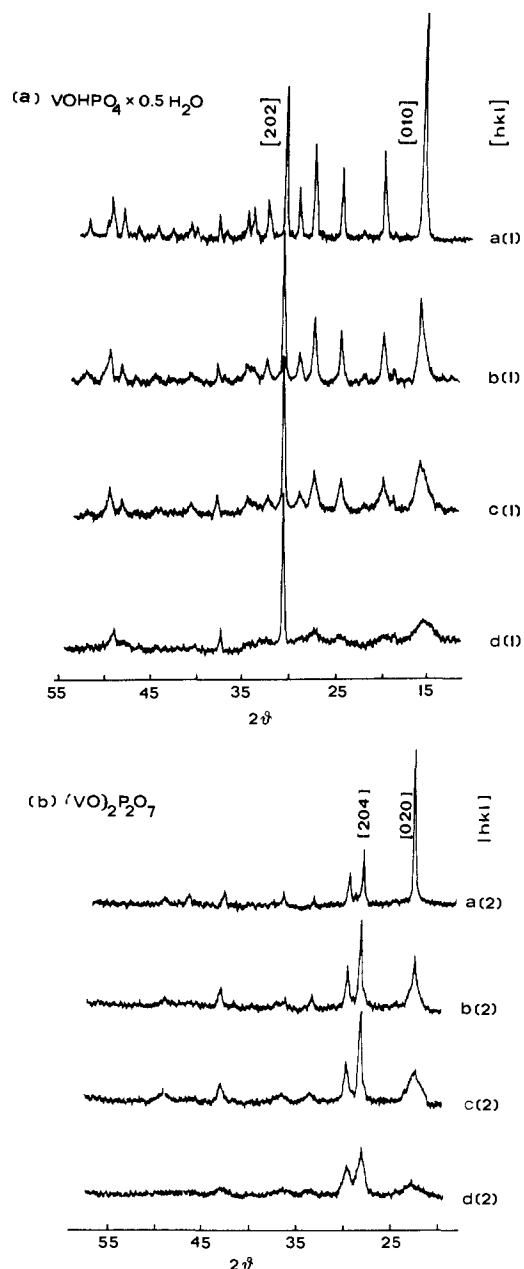
Figure 22. X-ray diffraction patterns[96] of vanadyl hydrogen phosphate (a) and of vanadyl pyrophosphate (b) for catalysts with P:V = 1.0 from different types of preparations.
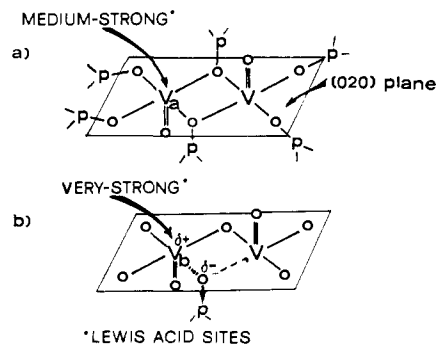
Figure 23. Model of Lewis acid sites[105] in vanadyl pyrophosphate with different degrees of disorder in the stacking fold of (020) planes: (a) medium-strong Lewis acid sites, well crystalline structure; (b) very strong Lewis acid sites, disordered crystalline structure.
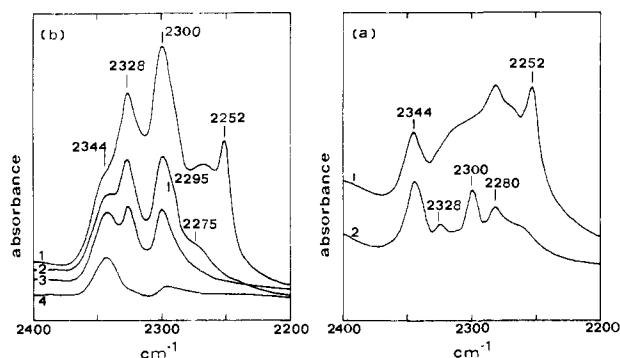
Figure 24. Fourier transform infrared spectra of acetonitrile adsorption[164] and different evacuation treatments on catalysts presenting different degrees of structural disorder: (a) well crystalline structure; (b) high disorder in the stacking fold of (020) planes of vanadyl pyrophosphate. a(1) and b(1), acetonitrile adsorbed at room temperature; a(2) and b(2), subsequent evacuation at room temperature; b(3) evacuation at 390 K for 10 min; b(4) evacuation at 430 K for 10 min. Acetonitrile gives coordination adducts with exposed coordinatively unsaturated cations with formation of two bands (in this region) due to (i) Fermi resonance between the C≡N stretching (ν_{CN}) and (ii) the combination of symmetric CH_3 deformation and C—C stretching (δ_{CH_3} + ν_{CC}). On (b) catalyst the two bands of equal intensities at 390 K (2328 and 2300 cm⁻¹) were assigned to coordinatively bonded acetonitrile on very strong Lewis sites. On (a) catalyst the two bands at 2280 and 2300 cm⁻¹ were attributed to coordinatively bonded acetonitrile on medium-strong Lewis sites.

mode of preparation. Busca et al.[96] have shown that in the vanadyl pyrophosphate it is possible to introduce structural defects (in particular, disorder in the stacking fold of (020) planes) modifying the catalyst precursor phase (hemihydrated vanadyl hydrogen phosphate) due to the topotacticity of the transformation. This is clearly shown, for example, in the comparison of X-ray diffraction patterns of different $VOHPO_4 \cdot 0.5H_2O$ and of corresponding $(VO)_2P_2O_7$.[96] The same strong broadening of the reflections of topologically equivalent (010) and (020) planes is shown[96] (Figure 22). Due to the topotactic transformation that occurs without the breaking of V–O–P connections and due to the higher electronegativity of P with respect to V, the presence of defects in the structure of vanadyl pyrophosphate is reflected on the surface in an enhancement of Lewis acidity of surface unsaturated vanadium ions (Figure 23).[105] Acetonitrile adsorption followed by FT-IR spectroscopy (Figure 24)[163,164] has been used to characterize the presence of different Lewis acid sites (medium strong and very strong) and to correlate their presence on the surface with the structural and catalytic properties of vanadyl pyrophosphate.[105,164] Strong-acid sites on $(VO)_2P_2O_7$ were observed also by Puttock and Rochester[167,168] with infrared spectroscopy and by Ai[42] with chemical tests. The presence of defects in the vanadyl pyrophosphate and their role in the rate of n-butane depletion were recently reported by Johnson et al.,[111] who quantitatively correlated the amount of defects (determined with magnetic susceptibility measurements) and the rate of butane depletion.

We may summarize all these observations in the following model: the presence of defects in the crystalline structure creates strain in the V–O–P bonds and would create a surface-activated reactive couple

$$[V^{\delta+}\cdots O^{\delta-} \to P] \qquad (10)$$

This reactive couple was proposed by Centi and
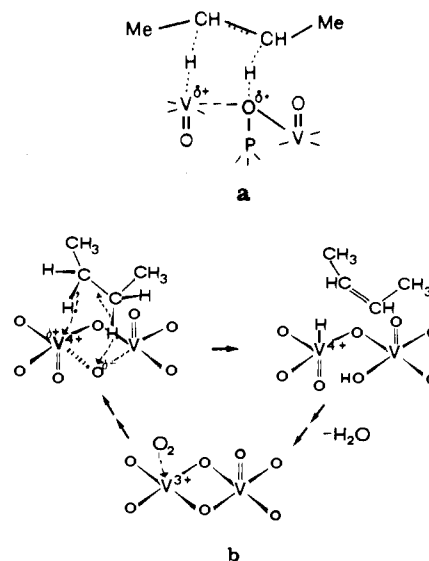
Figure 25. Proposed mechanism[105,165] of n-butane activation on vanadyl pyrophosphate catalysts: (a) detail of the concerted mechanism of 2 H abstraction; (b) redox cycle involved in the mechanism of activation.

Trifirò[165] as being responsible for the concerted mechanism of the removal of two hydrogen atoms, according to the scheme reported in Figure 25a. Figure 25b shows the redox cycle proposed for this mechanism of activation of n-butane.[105] The model is based on the idea that V^{IV}-oxygen reactive couples are the active sites of butane dehydrogenation.

Finally, V^V ions, on the contrary, are proposed by Hodnett and Delmon[38-40] on the basis of pulse reactor experiments showing high selectivities even in the absence of gaseous oxygen. Volta et al.[117] indicate that strong-acid centers are responsible for an H⁻ abstraction from butane, suggesting that these acid centers are V^{5+} ions in an amorphous surface phase with a high density of PO_4 tetrahedra around the vanadium octahedra. An increase of local surface phosphorus concentration increases the acidity of vanadium.

In conclusion, there are still several questions open in the literature about the nature and mechanism of the reaction of n-butane activation, notwithstanding the recent effort in this direction. This is an exciting field of research, allowing the possibility of the discovery of new pathways of selective activation of alkanes (a very open problem) and new reactions for functionalization of these poorly reactive hydrocarbons. Fundamental research on this aspect is necessary, in particular to solve the principal problem, whether the adsorbed activated oxygen species or the catalyst surface is the active species for the selective abstraction of hydrogen from the paraffinic C–H bond.

VIII. Role of Adsorbed and Lattice Oxygen Species

Steady-state and transient experiments (section III) have shown that the reaction from n-butane to maleic anhydride can be expressed in a stepwise manner, with intermediate formation of butenes, butadiene, and furan. Different reaction types are involved in these steps, i.e., activation of the alkane hydrocarbon, allylic dehydrogenation, 1,4-oxygen insertion on conjugated di-

olefins, and electrophilic oxidation of the furan ring.[64,104] It seems probable that different active sites and types of oxygen species are implicated in this polyfunctional behavior of the vanadyl pyrophosphate catalyst. In order to clarify this aspect, in this section we analyze some aspects of the mechanisms of these single steps and the types of oxygen species that may be involved.

Three types of lattice oxygen species with different reactivities are present at the surface of vanadium phosphorus oxides (Figure 1):

$$V = O \qquad V \diagdown_{\underset{|}{O}}^{\diagup} V \qquad V \diagdown_{\underset{P}{\overset{|}{O}}}^{\diagup} V \qquad (11)$$
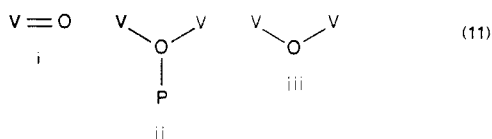
The participation of lattice oxygen is a general characteristic of metal oxide catalyzed reactions in selective hydrocarbon oxidation.[169] Over the past years it has been identified[170,171] for bismuth molybdate catalysts that different lattice oxygens are involved in the (i) α-H abstraction and (ii) the oxygen insertion mechanisms for propylene transformation to acrolein. The α-H abstraction occurs by oxide ions bridging bismuth and molybdenum atoms, whereas the oxygen insertion into the allylic intermediate originates from oxide ions associated only with molybdenum.[170] Similarly, different lattice oxide ions in vanadium phosphorus oxide may be necessary to achieve the polyfunctional behavior of these catalysts.[64]
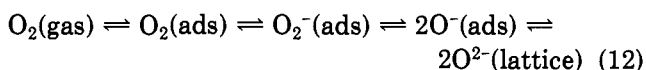
On the other hand, a series of equilibria with oxygen in the gas phase are established in which different species of adsorbed oxygen may form, gradually enriched with electrons by interaction with surface ions until the state of O^{2-}(lattice oxygen) is attained.[157,172]

$$O_2(gas) \rightleftharpoons O_2(ads) \rightleftharpoons O_2^-(ads) \rightleftharpoons 2O^-(ads) \rightleftharpoons$$
$$2O^{2-}(lattice) \quad (12)$$

For example, the O_2^- species is formed by interaction of the precursor $O_2(ads)$ with V^{4+} ions on the surface, donation of the electron being made from either the d_{yz} or the d_{zx} orbitals of the vanadium ion to an antibonding orbital of the oxygen atom. These are symmetry-allowed reactions.

In addition, these activated oxygen species may have different geometries and electronic structures, with the molecular axis being parallel or vertical to the interface.[63] This weakly bonded V^{4+}–O_2^- linear oxygen species was suggested to be active in the case of benzene conversion to maleic anhydride on vanadium-based catalysts.[173] In the process of transformation from O_2 to $2O^{2-}$, the characteristics of the oxygen species change from electrophilic (O_2^-) to the nucleophilic (O^{2-}) properties of lattice oxygen. Furthermore, in going from the alkane to maleic anhydride through the alkenes, a change of the possible point of attack of the oxygen species on the organic molecule is likely.

The first attempt to rationalize the problem of types of oxygen species involved in the mechanism of C_4 alkene transformation to maleic anhydride was reported by Weiss et al.[174] Vanadium–oxygen double bonds (V=O) were suggested to be the active sites both (i) in the oxydehydrogenation step from butenes to butadiene and (ii) in the consecutive steps of oxygen insertion to maleic anhydride. The first step involves a homolytic

SCHEME II. Reaction Pattern Proposed by Weiss et al.[174] for Butene Conversion to Maleic Anhydride
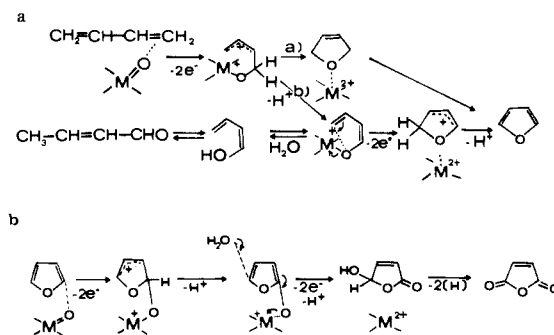

(C–H) dissociation of the adsorbed olefin and formation of the allyl radical coordinated to a metallic transition ion as a surface π-allyl complex. The allyl carbocation obtained can form the diene by loss of a proton through reaction with a nucleophilic agent (like an anion of the lattice). The allyl "ester" that forms can undergo a rapid reversible rearrangement in which each end of the carbon of the skeleton is alternatively bonded to the lattice oxygen. This lattice oxygen possesses a weak electrophilic reactivity. On the contrary, an electrophilic oxygen must be involved in the attack on the diene. The proposed mechanism is reported in Scheme 2a. The product of attack on the diene can occur according to two selective pathways: (a) 1,4-cyclization to 2,5-dihydrofuran, which is easily dehydrogenated to furan; (b) deprotonation of the allyl carbocation to a dienolate structure. Heterocyclization of this structure by a new intramolecular electrophilic attack leads to furan. The second path, however, can also form crotonaldehyde by hydration and retroaldolization, leading to a possible reduction in selectivity. An analogous mechanism may be assumed for the further oxidation to maleic anhydride, i.e., electrophilic attack, deprotonation, etc. (Scheme 2b).

The mechanism proposed by Weiss et al.[174] is only speculative, but recently Centi and Trifirò[175] reported experimental evidence concerning this mechanism. These authors considered V^{5+}=O as sites of oxygen insertion and V^{4+}=O or bridged V^{4+}—O—P as sites of allylic H abstraction. Figure 26 shows that by controlling the availability of oxygen it is possible to maximize the formation of furan from butadiene, obtaining very high selectivities to furan. Assuming a first-order rate equation for both the reaction from butadiene to furan and the reaction from furan to maleic anhydride and equal rate constants, the maximum yield of furan possible in a PFR reactor is around 30%.[137] This value is very close to the maximum yield of furan obtained on PVO catalysts.[175,176] This suggests that the reactivity of butadiene to furan and of furan to maleic anhydride is very similar. Figure 27 reports the comparison of the two reagents under the same conditions and the reactivity of but-1-ene in oxidative dehydrogenation (formation of butadiene) and of 2,5-dihydrofuran (DHF) in allylic dehydrogenation to furan. It is shown that the reactions of allylic dehydrogenation occur at very low temperatures, whereas the reactions of oxygen insertion on both butadiene and furan occur at higher temperatures. It should be noted that the reactions occur in the same range of temperatures and with similar selectivities to maleic anhydride
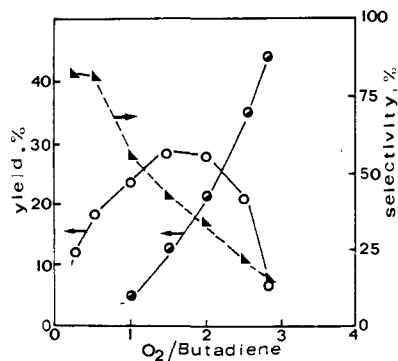
Figure 26. Effect of O_2/butadiene ratio at 330 °C in butadiene oxidation:[175] (O) furan yield; (⊙) maleic anhydride yield; (▲) furan selectivity. Feed: 0.8% butadiene.
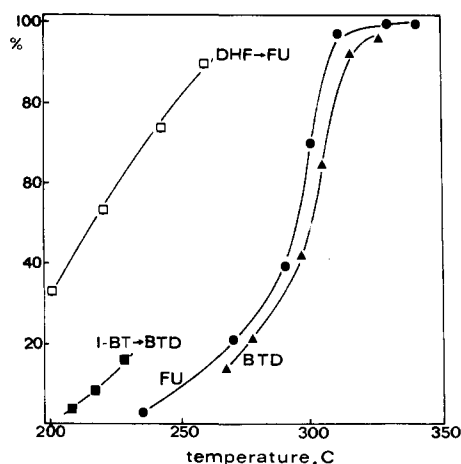
Figure 27. Comparison of reactivity of vanadyl pyrophosphate[104,175] in reaction of oxygen insertion (●, ▲) and allylic dehydrogenation (□, ■): (●) furan conversion; (▲) butadiene conversion; (■) but-1-ene conversion to butadiene; (□) dihydrofuran conversion to furan. Feed: 0.6% hydrocarbon, 12% oxygen.

(50–60%). This suggests that the nature of the reaction and of the active sites involved in the two reactions is very similar. On the other hand, due to the very high reactivity, the 2,5-dihydrofuran is quickly transformed to furan, which prevents its eventual detection as an intermediate of the reaction.

Further evidence is reported[177,178] in studies of the butadiene interaction with V^{5+}=O double bonds on a PVO catalyst with P:V = 1.0 using Fourier transform infrared spectroscopy (FT-IR). The formation of adsorbed products (with the most intense band centered near 1600 cm^{-1}) is observed[177] with simultaneous disappearance of a weak band at 2030 cm^{-1} attributed to the first overtone of $\nu_{V=O}$.[178] The interpretation of this effect (Scheme 3) is in agreement with the first step proposed by Weiss et al.[174]

Different indications, however, derive from the time-resolved experiments performed in the TAP reactor.[71,161] Special experiments were designed in order to detect the eventual formation of DHF. With DHF as the reactant in TAP experiments, at the point where maleic anhydride no longer can be made, DHF conversion drops off and only the formation of furan from DHF at about 30–50% conversion is detected. If the feed is switched at this point to butene or butadiene, only oxidative dehydrogenation from butene to butadiene and the formation of furan from butadiene are seen. No DHF is detected. Thus DHF is not com-

SCHEME III. Reaction Scheme Proposed by Busca et al.[177] in the Interaction of Butadiene with the V^{5+}=O Double Bond[a]

[a] This adsorbed species is stable and desorbs as crotonaldehyde only at temperatures about 100 °C higher than the reaction temperature.

pletely reacting on this surface, and yet it is not seen from these other reactants.

The alternative stepwise mechanism of double-H removal from 1,4-butadiene with subsequent nucleophilic O insertion seems also very unfavorable, due to the fact that the H atoms in the 2,3-positions of butadiene are more reactive. TAP experiments,[71] however, agree with steady-state and pulse reactor tests in the absence of O_2,[136,175] indicating lattice oxygen is involved in this step. Thus, the possible electrophilic addition of the activated oxygen molecule to form the 1,4-molecular oxygen adduct that decomposes to furan and water seems unlikely. Experiments[161] pulsing $^{18}O_2$ and butene or butadiene and monitoring the furan-^{16}O and furan-^{18}O as a function of pulse number indicate that at the start of the pulsing, the initial furan formed with both hydrocarbons contained only ^{16}O. With continued pulsing the furan-^{16}O yield dropped and the furan-^{18}O yield increased. An estimate of the amount of oxygen inserted from the catalyst in forming furan-^{16}O indicates subsurface lattice oxygen does not participate.

Resuming, no clear indications are present in the literature on the step of the mechanism from butadiene to furan. It is worthy of note that the stability of the intermediate reported in Scheme 3 is very high and it desorbs under vacuum only at very high temperatures.[177] This suggests that it cannot desorb as the DHF intermediate, but remains strongly bound to the surface up to final formation of furan (route b of Scheme 2a), which may desorb as an intermediate in the vacuum conditions of TAP experiments. All the experimental evidence agree that in the butadiene transformation to furan surface lattice oxygen is involved and the consecutive elementary reactions occur on intermediates strongly interacting with the catalyst surface. This interaction prevents possible desorption.[177]

Discordances are present in the literature about the consecutive step from furan to maleic anhydride. The data of Centi and Trifirò[139,175] suggest that the same kind of oxygen species is involved in the two reactions and thus lattice oxygen also is used in the transformation of furan to maleic anhydride. Pulse reactor tests[39,40,116,120,124,127,129] clearly indicate that lattice oxygen may be sufficient for the synthesis of maleic anhydride from both butenes and butane. Results of Morselli et al.,[132] furthermore, suggest that on a pure vanadyl pyrophosphate phase only oxidative dehydrogenation occurs, whereas in the presence of V^V the transformation to maleic anhydride even in the absence of O_2 may occur.

TAP experiments, however, suggest the different idea[71,161] that while butene and butadiene are readily converted to furan on a partially oxidized surface, furan is not readily converted to maleic anhydride. In a series of multipulse experiments in which anaerobic feeds of
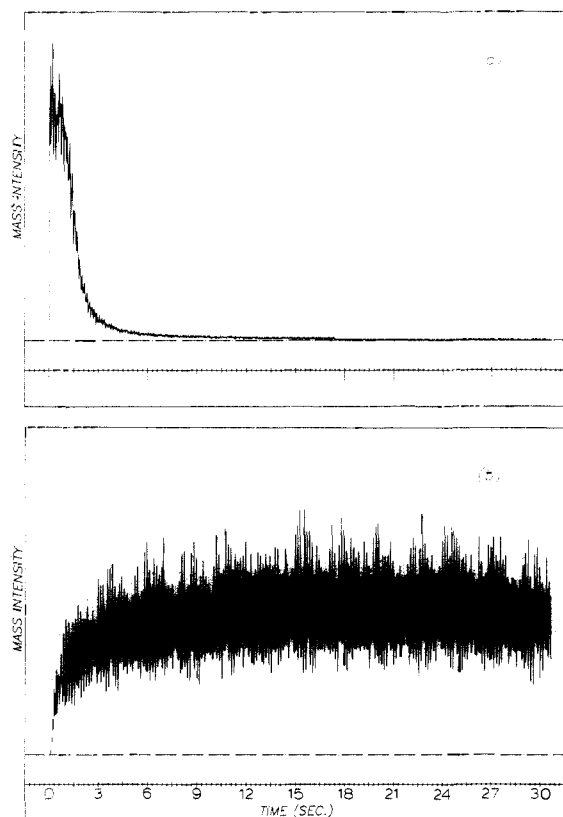
Figure 28. Multipulse format (40 pulses s^{-1}) data over (VO)$_2$P$_2$O$_7$ at 420 °C under anaerobic conditions[71] showing (a) maleic anhydride production from furan and (b) furan production from cis-but-2-ene.

Figure 29. Double-pulse data[71] showing (a) the CO$_2$ production and (b) the maleic anhydride production when oxygen and furan are injected into the microreactor at different times. The (V-O)$_2$P$_2$O$_7$ surface had been equilibrated with 50 pulses of oxygen and furan before those data were collected.

butene, butadiene, or furan were pulsed over preoxidized equilibrated (VO)$_2$P$_2$O$_7$ catalyst, the production of maleic anhydride from the furan and furan from olefins was monitored. Figure 28a shows how the maleic anhydride yield rapidly decreases as furan is pulsed through the reactor. The valve pulse rate is 40 pulses s^{-1} and within 2 s or 80 pulses the maleic anhydride yield is essentially zero. The furan yield (Figure 28b) obtained from pulsing butene into the same catalyst under identical conditions is initially zero, but rises to a maximum and then continues at that level for the duration of the pulsing. If the maleic anhydride yield is followed during butene pulsing, it closely resembles that observed during furan addition. Thus, under anaerobic conditions the oxygen which can readily oxidize furan is more rapidly depleted than the oxygen available to form furan from butene. Importantly, it was further observed that a catalyst which had (O*) removed by the reaction of furan to maleic anhydride was no longer able to activate butane. It is also worth noting that γ-butyrolactone formation was never detected during C$_4$ olefin and furan oxidation in TAP transient experiments. This suggests that oxygen insertion on the 2,5-positions of furan occurs simultaneously. The multipulse experiments performed in the TAP reactor clearly indicate that the PVO catalyst functions with two types of oxygen. The first type is suggested to be the activated species (O*) formed by strong chemisorption of the electrophilic dioxygen molecule. This species is responsible for furan oxidation and butane activation. It is present in relatively low concentrations. The second type of oxygen is suggested
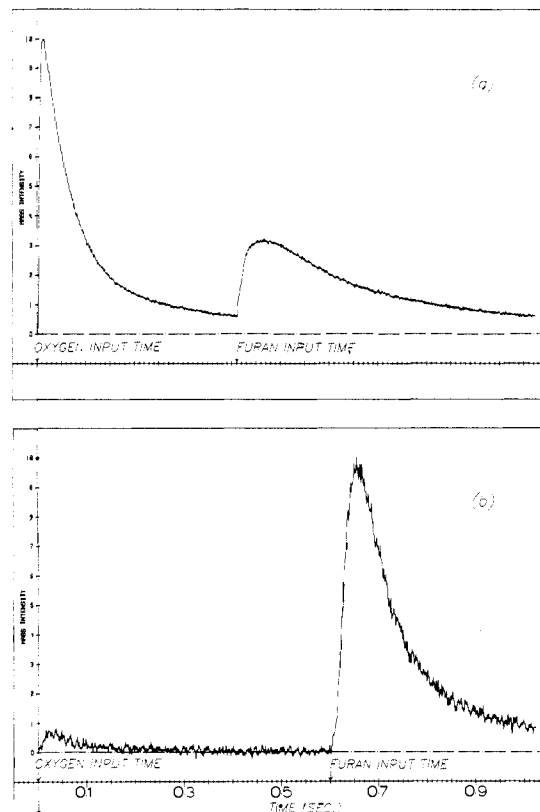
to be surface lattice oxygen (O$_{SL}$). It is responsible for the allylic oxydehydrogenation of olefins and for oxygen insertion with ring closure to form furan. The TAP results suggest that the selectivity of the butane oxidation reaction is influenced by the concentration of these species at the initial butane adsorption site. If insufficient oxygen is present then a partially oxidized species such as butene may desorb from the initial site and undergo oxidation at another site. This type of stepwise process would be less selective since butene is a less selective reactant than butane.

Nonselective reactions lead to the production of carbon oxides and to the formation of organic residues adsorbed on the catalyst surface. Double-pulse TAP experiments reveal a number of interesting aspects of this process. In a double-pulse experiment two reactants are pulsed into the reactor from different high-speed valves. The valves are synchronized, but are fired at different times. The interval between valve pulses can be varied from 0.1 μs to 1 s. The double-pulse results presented in Figures 29 and 30 were obtained on preoxidized base stock using oxygen and furan as the reactant feeds. Each TAP curve consists of 50 sets of pulses averaged together. The results reflect the state of the surface after it has been exposed to furan. On the first oxygen pulse no product was observed. After that both CO$_2$ and maleic anhydride were observed during the oxygen pulse. The feeds were adjusted so that the oxygen:furan ratio was 8:1. Figure 29a shows the CO$_2$ formation when the oxygen and furan pulses were separated by 400 ms. Two CO$_2$ peaks can be ob-
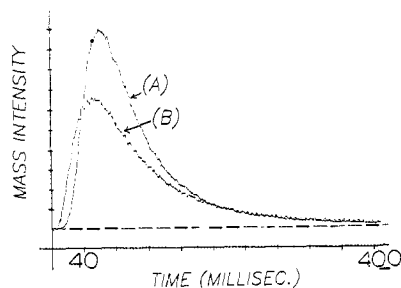
Figure 30. Comparison[71] of the maleic anhydride yield from double-pulse experiments during the furan injection period: (a) O_2/furan pulse separation was 0.1 ms; (b) O_2/furan pulse separation was 600 ms. The same vanadyl pyrophosphate catalyst was used in both experiments and the oxygen:furan ratio was 8:1 in both cases.

MALEIC ANHYDRIDE REACTION NETWORK

served. The larger one coincides with the oxygen pulse and the other with the furan pulse. The CO_2 data should be compared with the maleic anhydride data displayed in Figure 29b. The oxygen and furan pulses were separated by 600 ms. In this case the highest maleic anhydride yield coincides with the furan pulse and is about 50 times greater than that produced when oxygen is introduced. Moreover, if the order of the feed pulses is reversed and the interval between the two pulses is decreased, the size of the maleic anhydride pulse coinciding with the oxygen injection does not increase appreciably. These results indicate that the maleic precursor formed in the furan reaction has a relatively short lifetime. They also suggest that the reaction sequence is oxygen activation followed by furan oxidation and not vice versa. In addition, they show that even on a highly oxidized surface under differential conditions a portion of the furan oxidation is nonselective. In contrast, the size of the maleic anhydride peak obtained coinciding with the furan injection in a double-pulse experiment is dependent on the length of the interval between the oxygen and furan pulses. This is illustrated in Figure 30. Curve A is the maleic anhydride formation when the interval is 0.1 ms and curve B is the yield when the interval is 600 ms. In each case only the maleic anhydride peak which coincides with the furan injection is displayed. The reaction conditions for both curves were identical. These results show that the maleic anhydride yield was significantly smaller when the interval between the pulses was 600 ms. This indicates that other reaction channels were competing with furan for the activated oxygen. It is important to note that the maleic anhydride yield did not continuously decrease as the interval between the pulses was extended beyond 600 ms. This suggests an appreciable lifetime for one form of (O*) which is selective in maleic anhydride synthesis. Enhanced maleic yield upon decreasing pulse separation suggests a second selective oxygen (O*) form which is short-lived. Double-pulse TAP experiments[161] pulsing a mixture of ^{18}O/butene through an equilibrated $(VO)_2P_2O_7$ catalyst and monitoring the CO_2 temporal curves of the various isotopes suggest that the short-lived form of chemisorbed oxygen is also involved in the direct reaction with hydrocarbon to form CO_2. However, lattice oxygen plays a significant role in producing CO_2 by a much slower process. It also was suggested from the TAP experiments[71] that oxygen surface mobility is very high, although it seems likely that movement of oxygen is primarily through the
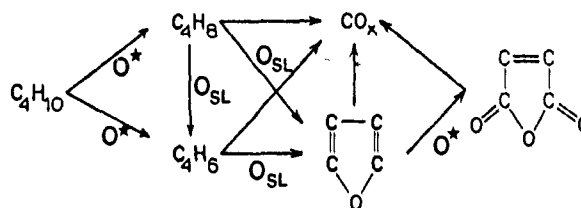
surface lattice. The TAP results are summarized in Scheme 4.

The role of adsorbed oxygen was investigated also by infrared spectroscopy.[41,177,179,180] Puttock and Rochester[179] studying the adsorption of C_4 hydrocarbons on the surface of vanadyl pyrophosphate found the formation of an adsorbed species under anaerobic conditions interacting with coordinatively unsaturated exposed vanadium cations. This species transforms to adsorbed maleic anhydride in the presence of gaseous oxygen. Similar observations with a different interpretation of the nature of the intermediate are reported by Busca et al.[177] for both butane and butadiene. These data agree with the TAP observations. It is worthy of note that recent quantitative EPR studies on PVO catalysts[181] have shown that under the usual vacuum pretreatment conditions (around 300–400 °C at 10^{-5} Torr), the fresh vanadyl pyrophosphate reduces, forming V^{3+} that in the presence of oxygen rapidly reoxidizes even at room temperature. This suggests that under vacuum conditions the surface of fresh PVO catalyst is strongly reduced, as confirmed from UV–vis diffuse reflectance spectra. The admission of O_2 thus causes a rapid reoxidation to V^{4+} and V^{5+}. However, in the TAP experiments it was found that allowing a preoxidized catalyst to sit 16 h under vacuum overnight at 420 °C did not result in a significant decrease in yield of maleic anhydride from furan. The long-lived chemisorbed oxygen, therefore, must not be easily removed from the surface of an equilibrated $(VO)_2P_2O_7$ catalyst.

Summarizing, the discordances found in the literature about the nature of the active species in the synthesis of maleic anhydride may be interpreted in light of what we concluded about the different kinetic behaviors of fresh and equilibrated catalysts. In the fresh catalysts lattice oxygen is very easily lost due to defects in the structure. This oxygen can be removed by simple evacuation. This explains why direct oxidization of the hydrocarbon to maleic anhydride can occur even in the absence of gaseous oxygen on a fresh PVO catalyst. With an equilibrated catalyst, lattice oxygen is not as labile and can perform only reactions of allylic oxydehydrogenations and of oxygen insertion with ring closure to form furan. In order to synthesize maleic anhydride or to activate the paraffin in an equilibrated catalyst, it is necessary to have gaseous oxygen interacting with the vanadyl pyrophosphate surface to form a long-lived oxidized surface vanadium oxo species. It is very probable that this species would correspond to an intermediate situation between simple activated

adsorbed oxygen like O_2^- or O^- species and lattice oxygen. Recent TAP results[71] suggest also that both this long-lived adsorbed oxygen species and lattice V^{5+} species are selective in maleic anhydride synthesis, but the adsorbed oxygen species reacts faster. In conclusion, it is clear that despite the complexity of this reaction, some advances have been made to single out the nature of the oxygen species involved in the different steps and in outlining the working state of catalyst. Substantial differences with respect to other reactions of selective oxidation, such as propylene to acrolein, have been suggested, in particular the role of electrophilic oxygen species in some steps of the mechanism. However, a number of contradictory aspects must be still solved for a more precise understanding of the individual steps in the complex reaction network, in particular regarding the nature of active oxygen species involved in the transformation of butadiene to maleic anhydride.

IX. Nature and Mobility of Adsorbed Species

Among the other themes on the mechanism of n-butane oxidation, this has been investigated in less detail. The first attempt to study the nature of the adsorbed species using infrared spectroscopy was reported by Rozhkova et al.[180] These authors investigated the chemisorption at 150 °C of butenes on a supported PVO catalyst (P:V = 1.0). Reversible chemisorption was characterized by the C=C bond forming a π complex and a weakening of the C–H bonds of the methyl group. The intensities of these effects depend on the surface state of the PVO catalyst. A prereduction treatment in a butene atmosphere at 400 °C and subsequent evacuation increase the effect on the methyl group, decreasing that on the C=C double bond. Weakening of the C–H bond in the methyl group was considered a necessary stage for their oxidation with initial formation of a butenyl radical. Rozhkova et al.[180] also observed that but-1-ene isomerizes easily to but-2-ene due to surface Brønsted sites (P–OH). Irreversible chemisorption, characterized by a band near 1600 cm^{-1}, was interpreted as the formation of a surface carbonate or oxalate structure coordinated to the catalyst surface atoms; these complexes are products of destructive transformation of butenes and are a source of formation of carbon oxides.

A more recent infrared study of the adsorption of butane, but-1-ene, buta-1,3-diene, furan, and maleic anhydride on the surface of anhydrous vanadyl pyrophosphate was reported by Puttock and Rochester.[179] Contact between butane vapor and $(VO)_2P_2O_7$ at temperatures up to 450 °C did not give rise to infrared bands due to adsorbed species. But-1-ene, on the contrary, gave rise to the formation of adsorbed species by contact at room temperature. Higher temperatures (200 °C) catalyzed the transformation of but-1-ene to but-2-enes, confirming the high surface acidity of these catalysts.[163,164,167,168] After removal of the gas phase an adsorbed species, characterized by a strong band near 1600 cm^{-1} and bands in the 2800–3000-cm^{-1} region, was observed. The latter bands, ascribed to saturated hydrocarbon groups, disappeared at higher temperatures (350 °C), whereas the band near 1600 cm^{-1} remained. This band was also observed by Rozhkova et al.[180] and

assigned to surface carbonate, whereas it was attributed by Puttock and Rochester[179] to a surface carboxylate. A similar spectrum of adsorbed species was found in the interaction of furan with the catalyst. The primary interaction between furan and the $(VO)_2P_2O_7$ was suggested to involve coordination between the oxygen atoms of associatively adsorbed furan molecules and coordinatively unsaturated exposed vanadium cations with Lewis acid properties. Furan showed slight oxidation to maleic anhydride in the absence of oxygen, but the presence of oxygen promoted maleic anhydride formation. Maleic anhydride was primarily nondissociatively adsorbed on $(VO)_2P_2O_7$, but two further bands at 1560 and 1450 cm^{-1}, attributed to carboxylate anions, suggested a partial oxidation of the adsorbed maleic anhydride.

Wenig and Schrader[41] studied with infrared spectroscopy the n-butane interaction with PVO catalysts with variable P:V atomic ratio (0.9, 1.0, and 1.1). These authors used an in situ FT-IR cell. Interaction of n-butane at temperatures higher than 300 °C led to the appearance of typical stretching frequencies of the carbonyl group of maleic anhydride (bands at 1179 and 1848 cm^{-1}, ν_{as} and ν_{sym}, respectively) and supposed $\nu_{C=O}$ of maleic acid (1725 cm^{-1}). Intensities of these bands increased as a function of the time in the in situ experiments. At lower temperatures (200 °C) a weak band (2979 cm^{-1}) was attributed to $\nu=_{CH_2}$ of an adsorbed olefinic species. In addition, at higher temperatures (400 °C) for catalysts with P:V = 1.0 and 1.1, further bands at 3010 and a 1570 cm^{-1} were assigned to $\nu=_{CH}$ and $\nu_{C=C}$ of an adsorbed cyclobutene species or a π-allyl surface complex. In addition, infrared bands of adsorbed carbon oxides, water, and n-butane were detected. In conclusion, these authors[41] presented evidence for the presence of reactant (n-butane), partially oxidized product (maleic anhydride), combustion products (CO, CO_2, H_2O), and reactive surface species (maleic acid and olefins) on the vanadyl pyrophosphate.

All the spectra reported by these authors were poorly resolved and lacking in quantitative data on the intensities of the bands. It is thus very difficult to make a comparison of these infrared results, even if qualitative general aspects of the spectra seem comparable. Interpretation of the nature of these adsorbed species is very different; sometimes unreliable assignment of the bands was made, and no support experiments to aid in the interpretation, as for example with labeled molecules, are given. More rigorous experiments are necessary in order to discern the nature of adsorbed species present on the surface and their relationship with the mechanism of reaction. It should be also stated that the Wenig and Schrader[41] observation of increased intensities of these bands as a function of time on stream during in situ experiments does not support their assignment to reactive surface intermediates. Turnover number of these species must be high, making their surface concentration independent of time on stream, at least on the time scale (1–4 h) they report. The formation of strongly adsorbed species was detected in pulse reactor tests[127,129,131,136,177] from the loss of carbon balance and in the TAP transient experiments.[71,161] In particular, in the pulse redox studies[129] it was observed that on the surface of vanadyl pyrophosphate during n-butane conversion under anaerobic conditions, strongly adsorbed species form that do not
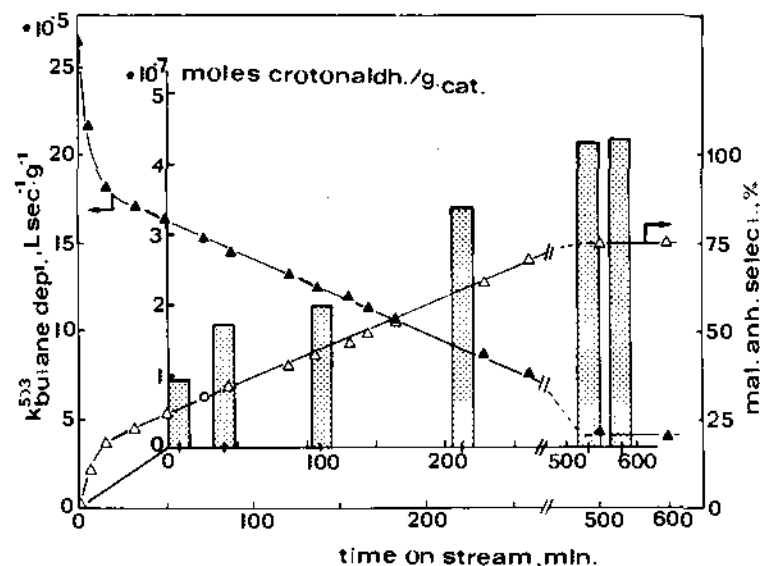
Figure 31. Effect of time on stream[177] on the rate constant of n-butane depletion at 300 °C (▲) and on the selectivity to maleic anhydride (△). The figure reports also the amount of crotonaldehyde found in parallel experiments during high-temperature thermal desorption ("stopped-flow desorption" experiments[177]) for a vanadyl pyrophosphate catalyst conditioned at 300 °C for different times on stream (flow of 1% n-butene, 12% O₂, 87% He).

desorb at the reaction temperature (400 °C). Sending pulses of pure O₂, in fact, the formation of carbon oxides, was observed, and the amount shows a maximum as a function of the number of pulses. [18]O pulse tests suggest that these strongly adsorbed species are significantly oxidized and that the combustion of this material is preceded by the reoxidation of the catalyst surface. A significant implication of these results is that the migration/exchange of the oxygen-containing species in the surface layer is faster than the oxidation of these adsorbed species.

Similar conclusions may be obtained on the basis of TAP transient experiments using multipulse experiments,[71,161] which also suggest that oxygen mobility of the surface top layer is very high, and the mobility of bulk oxygen is very low.

More precise information about the nature of these strongly adsorbed species in n-butane oxidation under steady-state conditions and a discussion of their implication in the catalytic behavior were presented by Busca et al.[177] These authors applied a different technique in order to characterize the nature of these products using "stopped-flow desorption" experiments. This technique consists of the quantitative determination of the nature of the products of thermal desorption from a catalyst surface after switching from steady-state conditions (flow of butane/air at around 300 °C) to those for desorption in deoxygenated anhydrous helium flow. Weakly bonded surface species were removed from the catalyst surface by flushing with helium. The more relevant aspect observed with this technique was the determination of high amounts of crotonaldehyde in the products of desorption, together with the presence of C₄ olefins and maleic anhydride. The latter two products, even if strongly bonded to the surface, may desorb at the temperature of the catalytic reaction (around 300 °C), whereas crotonaldehyde was found to only desorb at temperatures about 100 °C higher. This shows that the adsorbed organic molecule–surface complex that desorbs as crotonaldehyde is very stable on the surface, i.e., its turnover number is very low. The presence of this species was evidenced both in the presence and in the absence of gaseous oxygen and from

both butane and butadiene. Parallel FT-IR tests suggest that in the presence of gaseous oxygen this species may slowly transform to carbon oxides and maleic anhydride. The amount of this species on the surface of vanadyl pyrophosphate was found to increase as a function of time on stream. Parallel decreases in the rate of n-butane depletion and increases in the rate of maleic anhydride formation (Figure 31) were observed. The formation of this strongly bound species thus modifies the working state of $(VO)_2P_2O_7$ in steady-state reaction conditions for n-butane oxidation.

In conclusion, only fragmentary information is currently available in the literature on the important aspects of the nature of adsorbed species, the energetics of their interaction with vanadyl pyrophosphate, and the analysis of their importance in the mechanism of reaction relative to the dynamics of the working state of the catalyst surface. However, the literature does present important hypotheses and data on certain characteristics of this catalytic system. Strongly adsorbed species substantially change the nature of vanadyl pyrophosphate during steady-state oxidation of butane.[177] On the other hand, both transient[71,134,161] and labeled-molecule pulse redox experiments[129] suggest the dynamic nature of the surface layer with respect to oxygen and hydrogen exchange/migration. All these observations agree with the hypothesis[129] that the catalytic process in this complex reaction involves the shuttling of hydrogen away from and oxygen toward the intermediate adsorbed on the surface, and the intermediate forms a stable surface species which does not desorb, or reacts to form maleic anhydride. This mechanism is a key to the selectivity and the absence of intermediate products in the reaction of n-butane conversion to maleic anhydride.

X. Final Remarks

The 14-electron oxidation of butane to maleic anhydride is a very important reaction, both for commercial application and for scientific studies due to the inherent complexity of the mechanism. Two of its distinctive characteristics are (i) it is the only highly selective reaction of alkane functionalization and (ii) it is a very structure specific reaction. Notwithstanding extensive effort of many industrial catalysis research groups as well academic researchers, no other catalyst has been found that can match the selectivity of the vanadium phosphorus oxide system. This is in contrast to propene oxidation, where a number of different catalytic systems were found to be selective.[182–184] This speaks to the unique nature of the active-site requirements for n-butane activation and selective oxidation, as well as to the unparalleled mechanistic characteristics of this reaction. Butane can be activated, for example, on vanadium TiO₂-supported catalysts[105,156] (known selective catalysts for aromatic transformation to anhydrides), but only carbon oxides are formed. Similarly, the approach of Jung et al.[185] of creating coherent interfacial boundaries between the cleavage planes of an oxide active in dehydrogenation of butane into butenes (Co-MoO₄) with an oxide active for the transformation of butenes into maleic anhydride (MoO₃ supported on TiO₂) fails in obtaining a catalyst with the performance properties of PVO catalysts.

The vanadyl pyrophosphate catalyst, due to its particular crystalline structure, shows a singular ability to control its oxidizing power.[121,130] This demonstrates the importance of structural site isolation of oxidizing sites indicated by Grasselli et al.[130,140] as the key in the control of selectivity in partial selective oxidation reactions.

The best selectivity is achieved when desorption of less selective intermediates along the reaction coordinate is avoided because the olefin reactions are less selective on a highly active butane $(VO)_2P_2O_7$ catalyst. This implies that attempts to promote individual steps in the reaction sequence, such as oxidative dehydrogenation promoters to facilitate the formation of olefins, will not result in significantly better catalysts.

The availability of oxygen to the surface is critical in avoiding desorption of less selective olefins. Thus it would appear that major selectivity gains could be achieved if more oxygen could be channeled to the active site. Because of the dynamic response of the $(VO)_2P_2O_7$ surface to the redox potential of the feed, as demonstrated by the changes induced by hydrocarbon feeds of different concentrations, comparisons of literature results on the reaction of C_4 hydrocarbons with vanadium phosphorus oxide catalyst should be done with this in mind. Additional research on identifying and characterizing the surface and its dynamic response under reaction conditions, however, is needed in order to better understand these important aspects.

The different kinetic behavior found in but-1-ene and n-butane oxidation can be explained on the basis of the different reducing power of the two hydrocarbons. The but-1-ene requires a lower oxidation state of the catalyst surface as compared to n-butane. To optimize the valence state of the catalyst surface different reaction conditions may be necessary, in particular, a different ratio of hydrocarbon/O_2 concentrations. Thus, the best catalysts for the oxidation of the two hydrocarbons to maleic anhydride must be different, because the optimal redox properties required are different.

A central role in the modification of surface reactivity is adsorption of organic molecules and oxygen species. The mobility of these species under steady-state conditions of reaction is another characteristic of the vanadyl pyrophosphate catalyst in n-butane oxidation, but more detailed information is necessary on this central aspect of PVO surface reactivity.

The evidence leading to speculations on the catalytic behavior of PVO catalysts based only on the crystal chemistry aspects[73,123] may not be sufficient for analysis of the complex reaction of butane conversion. A discussion of the selectivity in oxidation reactions on mixed oxides must necessarily include a consideration of the dynamics of the process[130] comprising a three-phase system: (i) a gas phase, (ii) a solid phase, and (iii) a two-dimensional surface region at the interface. Just static or crystallographic approaches[123,186] cannot give a realistic picture of the working state of a catalyst and the mechanism of reaction.

These discussed characteristics of $(VO)_2P_2O_7$ are utilized in the design of the process of n-butane conversion in a transport bed reactor.[22] In this two-stage reactor, the catalyst surface can be charged with oxygen prior to butane reaction and in the butane leg of the reactor maleic anhydride destruction is minimal because of low oxygen and limited backmixing. This would give

rise to the higher selectivities and yields realized in this process.

Activation of the alkane hydrocarbon is a further important aspect of this reaction because of its mechanistic relevance in the study of other heterogeneous reactions for functionalization of alkanes, and for the possible comparison with the well-known mechanisms of alkane activation in organometallic chemistry.[187] A very specific surface structure is needed, and it would seem that the binding of intermediates until product is formed (single-site process) is essential to high selectivities. For example, this means that in the oxidation of methane to formaldehyde,[188] the site must be capable of binding the methyl and methoxy intermediates during the process of oxidation to formaldehyde. It is likely that any paraffin selective oxidation catalyst will have to be as structurally unique and specific as $(VO)_2P_2O_7$.

Finally, the challenge of molecular level identification of the nature of the surface sites responsible for the individual steps of the transformation and of the elementary reactions involved remains. More research using more sophisticated chemical and spectroscopic surface techniques is needed to clarify a number of the ambiguous results. In this respect, a unique catalyst evaluation system like TAP with its real-time submillisecond resolution will enable investigations of the mechanism of complex reactions by using special reactants for chemical trapping of the intermediates of reaction, opening up a new dimension in the investigation of these types of complex catalytic reactions.

XI. References

(1) Malow, M. Hydrocarbon Process. 1980, 11, 149.
(2) Haase, H. Chem.-Ing.-Tech. 1972, 1-2, 80.
(3) Weissermel, K.; Arpe, H. J. Industrial Organic Chemistry; Verlag Chemie: Weinheim, New York, 1978.
(4) Kanetaka, J.; Asano, T.; Masamune, S. Ind. Eng. Chem. 1970, 62, 31.
(5) Chem. Mark. Rep. 1986, 230, 8.
(6) Ind. Chem. News 1986, 3, 9.
(7) Wohlfahrt, K.; Emig, G. Hydrocarbon Process. 1980, 6, 83.
(8) Wurzbacher, G. Chem.-Ing.-Tech. 1973, 22, 1297.
(9) De Maio, D. A. Chem. Eng. 1980, 5, 104.
(10) Budi, F.; Neri, A.; Stefani, G. Hydrocarbon Process. 1982, 1, 159.
(11) Arnold, S. C.; Sucire, G. D.; Verde, V.; Neri, L. Hydrocarbon Process. 1985, 9, 123.
(12) Varma, R. A.; Saraf, D. N. Ind. Eng. Chem. Prod. Res. Dev. 1979, 18, 7.
(13) Udovich, C. A.; Edwards, R. C. U.S. Patent 4564688 (to Amoco), 1986.
(14) Barone, B. J. U.S. Patent 4251390 (to Denka), 1981.
(15) Schneider, R. A. U.S. Patent 3864280 (to Chevron), 1975.
(16) Schneider, R. A. U.S. Patent 4043943 (to Chevron), 1977.
(17) Keppel, R. A.; Franchetti, V. M. U.S. Patent 4632915 (to Monsanto), 1986.
(18) Wrobleski, J. T.; Edwards, J. W.; Graham, C. R.; Keppel, R. A.; Raffelson, M. U.S. Patent 4562268 (to Monsanto), 1985.
(19) Dutta, S.; Arnold, S. C.; Sucire, G. D.; Verde, L. In Proceedings, 8th International Symposium on Chemical Reaction Engingeering (Edinburg, Sept 1984); Pergamon: Oxford, 1984; EFCE Series 37, p 517.
(20) Blum, P. R.; Nicholas, M. L. U.S. Patent 4317778 (to Sohio), 1982.
(21) Chem. Eng. News 1987, 2, 24.
(22) Contractor, R. M.; Bergna, H. E.; Horowitz, H. S.; Blackstone, C. M.; Malone, B.; Torardi, C. C.; Griffiths, B.; Chowdhry, U.; Sleight, A. W. Catal. Today 1987, 1, 49.
(23) Catalysis Today (Proceedings, 1st Symposium on New Developments in Selective Oxidation); Ruiz, P.; Delmon, B., Eds.; Elsevier: Amsterdam, 1987; Vol. 1, 2.
(24) Hodnett, B. K. Catal. Rev.—Sci. Eng. 1985, 27, 373.

(25) Hucknall, D. J. *Selective Oxidation of Hydrocarbons*; Academic: London, 1974.
(26) Cavani, F.; Centi, G.; Trifirō, F. *J. Chem. Soc., Chem. Commun.* **1985**, 492.
(27) Hodnett, B. K.; Delmon, B. *Appl. Catal.* **1983**, *9*, 203.
(28) Hodnett, B. K.; Permanne, Ph.; Delmon, B. *Appl. Catal.* **1983**, *6*, 231.
(29) Hodnett, B. K.; Delmon, B. *Bull. Soc. Chim. Belg.* **1983**, *92*, 695.
(30) Martini, G.; Morselli, L.; Riva, A.; Trifirō, F. *React. Kinet. Catal. Lett.* **1978**, *8*, 431.
(31) Bordes, E.; Courtine, P.; Johnson, J. W. In *Proceedings, 10th International Symposium on Reactivity of Solids* (Dijon, France, Sept 1984), p 512.
(32) Bordes, E.; Johnson, J. W.; Raminosona, A.; Courtine, P. *Mater. Sci. Monogr.* **1985**, *28B*, 887.
(33) Bordes, E.; Courtine, P. *J. Chem. Soc., Chem. Commun.* **1985**, 294.
(34) van Geem, P. C.; Nobel, A. P. P. *Catal. Today* **1987**, *1*, 5.
(35) Pyatnitskaya, A. I.; Komashko, G. A.; Zazhigalov, V. A. *Katal. Katal.* **1979**, *17*, 94. Pyatnitskaya, A. I.; Komashko, G. A.; Zazhigalov, V. A.; Gorokhovatskii, Ya. B. *React. Kinet. Catal. Lett.* **1977**, *6*, 341.
(36) Garbassi, F.; Bart, J. C.; Montino, F.; Petrini, G. *Appl. Catal.* **1985**, *16*, 271.
(37) Garbassi, F.; Bart, J. C.; Tassinari, R.; Vlaic, G.; Lagarde, P. *J. Catalysis* **1986**, *98*, 317.
(38) Hodnett, B. K.; Delmon, B. *J. Catal.* **1984**, *88*, 43.
(39) Hodnett, B. K.; Delmon, B. *Appl. Catal.* **1985**, *15*, 141.
(40) Hodnett, B. K.; Delmon, B. *Ind. Eng. Chem. Fundam.* **1984**, *23*, 465.
(41) Wenig, R. W.; Schrader, G. L. *Ind. Eng. Chem. Fundam.* **1986**, *25*, 612. Wenig, R. W.; Schrader, G. L. *J. Phys. Chem.* **1986**, *90*, 6480.
(42) Ai, M. *J. Catal.* **1986**, *100*, 336.
(43) Ai, M.; Boutry, P.; Montarnal, R. *Bull. Soc. Chim. Fr.* **1970**, *8–9*, 2775.
(44) Ai, M.; Boutry, P.; Montarnal, R.; Thomas, G. *Bull. Soc. Chim. Fr.* **1970**, *8–9*, 2783.
(45) Ai, M. *Bull. Chem. Soc. Jpn.* **1970**, *43*, 3490.
(46) Ai, M.; Suzuki, S. *Bull. Chem. Soc. Jpn.* **1974**, *47*, 3074.
(47) Nakamura, M.; Kawai, K.; Fujiwara, Y. *J. Catal.* **1974**, *34*, 345.
(48) Seeboth, H.; Kubias, K.; Wolf, H.; Lücke, B. *Chem. Tech. (Leipzig)* **1976**, *28*, 730.
(49) Seeboth, H.; Ladwig, G.; Kubias, B.; Wolf, G.; Lücke, B. *Ukr. Khim. Zh.* **1977**, *43*, 842.
(50) Bordes, E.; Courtine, P. *J. Catal.* **1979**, *57*, 236.
(51) Matsuura, I. *Hyomen* **1982**, *20*, 605.
(52) Shimoda, T.; Okuhara, T.; Misono, M. *Bull. Chem. Soc. Jpn.* **1985**, *58*, 2163.
(53) Morselli, L.; Riva, A.; Trifirō, F.; Zucchi, M.; Emig, G. *Chim. Ind. (Milan)* **1978**, *60*, 791.
(54) Poli, G.; Ruggeri, O.; Trifirō, F. In *Proceedings, 9th International Symposium on the Reactivity of Solids* (Krakōw, Poland, 1980), p 512.
(55) Emig, G.; Trifirō, F.; Hofmann, H. *Chem.-Ztg.* **1980**, *5*, 165.
(56) Poli, G.; Resta, I.; Ruggeri, O.; Trifirō, F. *Appl. Catal.* **1981**, *1*, 395.
(57) Lanzarini, G.; Trifirō, F.; Ruggeri, O. *Ann. Chim. (Paris)* **1981**, 461.
(58) Centi, G.; Galassi, C.; Manenti, I.; Riva, A.; Trifirō, F. In *Preparation of Catalysts III*; Poncelet, G., Grange, P., Jacobs, P., Eds.; Elsevier: Amsterdam, 1983; p 543.
(59) Centi, G.; Manenti, I.; Riva, A.; Trifirō, F. *Appl. Catal.* **1984**, *9*, 177.
(60) Cavani, F.; Centi, G.; Trifirō, F. *Appl. Catal.* **1984**, *9*, 191.
(61) Grasselli, R. K. In *Surface Properties and Catalysis by Non-Metals*; Bonnelle, J. P., Delmon, B., Derouane, E., Eds.; NATO ASI Series C.105; Reidel: Dordrecht, The Netherlands, 1982; pp 273, 289.
(62) Dadyburjor, D. B.; Jewar, S. S.; Ruckenstein, R. *Catal. Rev.—Sci. Eng.* **1979**, *19*, 293.
(63) Haber, J. In *Proceedings, 8th International Congress on Catalysis*, (Berlin, 1984); Dechema: Frankfurt am Main, 1984; Vol. I, p 85.
(64) Centi, G.; Trifirō, F. *Appl. Catal.* **1984**, *12*, 1.
(65) Kung, H. H. *Ind. Eng. Chem. Prod. Res. Dev.* **1986**, *25*, 171.
(66) Grasselli, R. K.; Burrington, J. D.; Brazdil, J. F. *Faraday Discuss. Chem. Soc.* **1981**, *72*, 203.
(67) Grasselli, R. K.; Burrington, J. D. *Adv. Catal.* **1981**, *30*, 133.
(68) Centi, G.; Trifirō, F.; Vaccari, A.; Pajonk, G. M.; Teichner, S. *J. Bull. Soc. Chim. Fr.* **1981**, *7–8*, 1.
(69) Cavani, F.; Centi, G.; Manenti, I.; Riva, A.; Trifirō, F. In *Proceedings, 9th Ibero-American Symposium on Catalysis* (Lisbon, Portugal, July 1984), p 973.
(70) Centi, G.; Fornasari, G.; Trifirō, F. *Ind. Eng. Chem. Prod. Res. Dev.* **1985**, *24*, 32.
(71) Gleaves, J. T.; Ebner. J. R.; Kuechler, T. C. *Catal. Rev.*, accepted.

(72) Ebner, J. R.; Gleaves, J. T. U.S. Patent 4 626 412 (to Monsanto Co.), 1986.
(73) Bordes, E. Preprints, ACS Symposium of Division of Petroleum Chemistry, "Hydrocarbon Oxidation", New Orleans Meeting, sept 1987.
(74) Jordan, B.; Calvo, C. *Can. J. Chem.* **1973**, *51*, 2621.
(75) Jordan, B.; Calvo, C. *Acta Crystallogr., Sect. B: Struct. Crystallogr. Cryst. Chem.* **1976**, *B32*, 2899.
(76) Gopal, R.; Calvo, C. *J. Solid State Chem.* **1972**, *5*, 432.
(77) Bhargava, R. N.; Condrate, R. A. *Appl. Spectrosc.* **1977**, *31*, 230.
(78) Ladwig, G. *Z. Anorg. Allq. Chem.* **1965**, *338*, 266.
(79) Seifer, G. B.; Tananaev, I. V. *Russ. J. Inorg. Chem. (Engl. Transl.)* **1963**, *8*, 521.
(80) Bordes, E.; Courtine, P.; Pannetier, G. *Ann. Chim. (Paris)* **1973**, *8*, 105.
(81) Ballutaud, D.; Bordes, E.; Courtine, P. In *Studies in Inorganic Chemistry*; Metselaar, R., et al., Eds.; Elsevier: Amsterdam, 1983; Vol. 3, p 512.
(82) Ballutaud, D.; Bordes, E.; Courtine, P. *Mater. Res. Bull.* **1982**, *17*, 519.
(83) Tachez, M.; Theobald, F.; Bordes, E. *J. Solid State Chem.* **1981**, *40*, 280.
(84) Tachez, M.; Theobald, F.; Bernard, J.; Hewat, A. W. *Rev. Chim. Miner.* **1982**, *19*, 291.
(85) Tietze, H. R. *Aust. J. Chem.* **1981**, *34*, 2035.
(86) Chernorukov, N. G. *Izv. Akad. Nauk. SSSR Neorg. Mater.* **1981**, *17*, 338.
(87) Chernorukov, N. G.; Egorov, N. P.; Korshunov, I. A. *Russ. J. Inorg. Chem. (Engl. Transl.)* **1978**, *23*, 1479.
(88) Johnson, J. W.; Jacobson, A. J.; Brody, J. F.; Rich, S. M. *Inorg. Chem.* **1982**, *21*, 3820.
(89) Johnson, J. W.; Jacobson, A. J. *Angew. Chem., Int. Ed. Engl.* **1983**, *22*, 412.
(90) Jacobson, A. J.; Johnson, J. W.; Brody, J. F.; Scanlon, J. C.; Lewansowski, J. T. *Inorg. Chem.* **1985**, *24*, 1782.
(91) Johnson, J. W.; Johnston, D. C.; Jacobson, A. J.; Brody, J. F. *J. Am. Chem. Soc.* **1984**, *106*, 8123.
(92) Leonowicz, M. E.; Johnson, J. W.; Brody, J. F.; Shannon, H. F.; Newsam, J. M. *J. Solid State Chem.* **1985**, *56*, 370.
(93) Bordes, E.; Courtine, P.; Johnson, J. W. *J. Solid State Chem.* **1984**, *55*, 270.
(94) Torardi, C. C.; Calabrese, J. C. *Inorg. Chem.* **1984**, *23*, 1308.
(95) Centi, G.; Trifirō, F.; Poli, G. *Appl. Catal.* **1985**, *19*, 225.
(96) Busca, G.; Cavani, F.; Centi, G.; Trifirō, F. *J. Catal.* **1986**, *99*, 400.
(97) Whitinghaum, M. S.; Jacobson, A. J., Eds. *Intercalation Chemistry*; Academic: New York, 1982.
(98) Beneke, K.; Lagaly, G. *Inorg. Chem.* **1983**, *22*, 1503.
(99) Dines, M. B.; Di Giacomo, P. M. *Inorg. Chem.* **1981**, *20*, 92.
(100) Alberti, G.; Costantino, U. *J. Mol. Catal.* **1984**, *27*, 235.
(101) Alberti, G.; Costantino, U.; Perego, G. *J. Solid State Chem.* **1986**, *63*, 455.
(102) Johnson, J. W.; Jacobson, A. J.; Brody, J. F.; Lewandowski, J. T. *Inorg. Chem.* **1984**, *23*, 3842.
(103) Zazhigalov, V. A.; Pyatnitskaya, A. I.; Bachetokova, I. V.; Komashko, G. A.; Ladwig, G.; Belousov, V. M. *React. Kinet. Catal. Lett.* **1983**, *23*, 119.
(104) Centi, G.; Trifirō, F. *Chim. Ind. (Milan)* **1986**, *68*, 74.
(105) Busca, G.; Centi, G.; Trifirō, F. *Appl. Catal.* **1986**, *25*, 265.
(106) Cavani, F.; Centi, G.; Trifirō, F.; Poli, G. *J. Thermal Anal.* **1985**, *30*, 1241.
(107) Cavani, F.; Centi, G.; Manenti, I.; Riva, A.; Trifirō, F. 187th National Meeting of the American Chemical Society (E. V. Murphee Award Symposium), St. Louis, April 1984.
(108) Gorbunova, Yu. E.; Linde, S. A. *Sov. Phys. Dokl.* **1979**, *24*, 138.
(109) Middlemiss, N. Thesis, McMaster University, Hamilton, Canada, 1978.
(110) Johnston, D. C.; Johnson, J. W. *J. Chem. Soc., Chem. Commun.* **1985**, 1720.
(111) Johnson, J. W.; Johnston, D. C.; Jacobson, A. J. Preprints, 4th International Symposium on the Scientific Bases for the Preparation of Heterogeneous Catalysts (Louvain-la-Neuve, Belgium, Sept 1986), p 85.
(112) Ladwig, G. *Z. Chem.* **1968**, *8*, 307.
(113) Moser, T. P.; Schrader, G. L. *J. Catal.* **1985**, *92*, 43.
(114) Buchanan, J. S.; Apostolakis, J.; Sundaresan, S. *Appl. Catal.* **1985**, *19*, 65.
(115) Khulbe, K. C.; Mann, R. S. *Acta Chim. Hung.* **1977**, *92*, 17.
(116) Martini, G.; Trifirō, F.; Vaccari, A. *J. Phys. Chem.* **1982**, *86*, 1573.
(117) Bergeret, G.; David, M.; Broyer, J. P.; Volta, J. C.; Hecquet, G. *Catal. Today* **1987**, *1*, 37.
(118) Volta, J. C. 19th Swedish Symposium on Catalysis (Lund, Sweden, Oct 1986).
(119) Bergeret, G.; Broyer, J. P.; David, M.; Gallezot, P.; Volta, J. C.; Hecquet, G. *J. Chem. Soc., Chem. Commun.* **1986**, 825.
(120) Cavani, F.; Centi, G.; Trifirō, F.; Vaccari, A. In *Adsorption and Catalysis on Oxide Surfaces*; Che, M., Bond, G. C., Eds.;

Elsevier: Amsterdam, 1985; p 287.
(121) Cavani, F.; Centi, G.; Riva, A.; Trifirò, F. *Catal. Today* **1987**, *1*, 17.
(122) Schneider, P.; Emig, G.; Hofmann, H. *Chem.-Ing.-Tech.* **1985**, *57*, 728.
(123) Courtine, P. In *Solid State Chemistry in Catalysis*; Grasselli, R. K., Brazdil, J. F., Eds.; American Chemical Society: Washington, DC, 1985; ACS Symp. Ser. 279, p 37.
(124) Zazhigalov, V. A.; Zaitsev, Yu. P.; Belousov, V. M.; Wüstneck, N.; Wolf, H.; Seeboth, H. *React. Kinet. Catal. Lett.* **1986**, *30*, 47.
(125) Wüsteck, N.; Wolf, H.; Seeboth, H. *React. Kinet. Catal. Lett.* **1982**, *21*, 497.
(126) Minow, G.; Schnabel, K. H.; Ohlmann, G. *React. Kinet. Catal. Lett.* **1983**, *22*, 399.
(127) Szakacs, S.; Wolf, H.; Mink, G.; Bertoti, I.; Wüstneck, N.; Lücke, B.; Seeboth, H. *Catal. Today* **1987**, *1*, 27.
(128) Zazhigalov, V. A.; Zaitsev, Yu. P.; Belousov, V. M.; Wüstneck, N.; Wolf, H. *React. Kinet. Catal. Lett.* **1984**, *24*, 375.
(129) Pepera, M. A.; Callahan, J. L.; Desmond, M. J.; Milberger, E. C.; Blum, P. R.; Bremer, N. J. *J. Am. Chem. Soc.* **1985**, *107*, 4883.
(130) Cavani, F.; Centi, G.; Trifirò, F.; Grasselli, R. K. Preprints, ACS Symposium of Division of Petroleum Chemistry, "Hydrocarbon Oxidation", New Orleans Meeting, Sept 1987.
(131) Cavani, F.; Centi, G.; Trifirò, F. *Appl. Catal.* **1985**, *15*, 151.
(132) Morselli, L.; Trifirò, F.; Urban, L. *J. Catal.* **1982**, *75*, 112.
(133) Centi, G.; Fornasari, G.; Trifirò, F. *J. Catal.* **1984**, *89*, 44.
(134) Buchanan, J. S.; Sundaresan, S. *Appl. Catal.* **1986**, *26*, 211.
(135) Wrobleski, J. T.; Brooks, R. F.; Ellis, W. S.; Mount, R. A. Monsanto Internal Report, 1982.
(136) Cavani, F.; Centi, G.; Manenti, I.; Trifirò, F. *Ind. Eng. Chem. Prod. Res. Dev.* **1985**, *24*, 221.
(137) Levenspiel, O. *Chemical Reaction Engineering*; Wiley: New York, 1972.
(138) Ebner, J. R.; Gleaves, J. T.; Kuechler, T. C.; Li, T. P. In *Chemicals from Syngas and Methanol*; Fahey, D., Ed.; American Chemical Society: Washington, DC, 1987; ACS Symp. Ser. 328, p 189.
(139) Cavani, F.; Centi, G.; Manenti, I.; Riva, A.; Trifirò, F. *Ind. Eng. Chem. Prod. Res. Dev.* **1983**, *22*, 565.
(140) Callahan, J. L.; Grasselli, R. K. *AIChE J.* **1963**, *9*, 755.
(141) Escardino, A.; Sola, C.; Ruiz, F. *An. Quim.* **1973**, *69*, 1157.
(142) Wohlfahrt, K.; Hofmann, H. *Chem.-Ing.-Tech.* **1980**, *52*, 811.
(143) Sharma, R. K.; Cresswell, D. L. Paper presented at AIChE Annual Meeting, San Francisco, Nov 1984.
(144) Lerou, J. J.; Weiher, J. F., Paper presented at Pittsburgh/Cleveland Catalysis Society Meeting, May 1986.
(145) Kruchinin, Yu. A.; Mischenko, Yu. A.; Nechiporuk, P. P.; Gel'stein, A. I. *Kinet. Katal.* **1984**, *25*, 392.
(146) Varma, R. L.; Saraf, D. M. *J. Catal.* **1978**, *55*, 361. Varma, R. L.; Saraf, D. M. *J. Catal.* **1978**, *55*, 361. Varma, R. L.; Saraf, D. M. *Indian J. Chem. Eng.* **1978**, *6*, 314.
(147) Brkic, D.; Trifirò, F. *Ind. Eng. Chem. Prod. Res. Dev.* **1979**, *18*, 333.
(148) Cavani, F.; Centi, G.; Trifirò, F. *Ind. Eng. Chem. Prod. Res. Dev.* **1983**, *22*, 570.
(149) Sunderland, P. *Ind. Eng. Chem. Prod. Res. Dev.* **1976**, *15*, 90.
(150) Hofmann, H.; Emig, G.; Röder, W. In *Proceedings, 8th International Symposium on Chemical Engineering*; Pergamon: Oxford, 1984; EFCE Series 37, p 419.
(151) Müller, B.; Baerns, M. *Chem.-Ing.-Tech.* **1980**, *52*, 826.
(152) Matsuura, I. In *Proceedings, 8th International Congress on Catalysis* (Berlin, 1984); Dechema: Frankfurt am Main, 1984; Vol. IV, p 473.
(153) Zein El Deen, A.; Baerns, M. In *Proceedings, 5th Ibero-American Symposium on Catalysis*, 1978, p 67.
(154) Mori, K.; Miyamoto, A.; Murakami, Y. *J. Phys. Chem.* **1985**, *89*, 4265.
(155) Aika, K.; Lunsford, J. H. *J. Phys. Chem.* **1977**, *81*, 1393. Takita, Y.; Lunsford, J. H. *J. Phys. Chem.* **1979**, *83*, 683. Iwamoto, M.; Lunsford, J. H. *J. Phys. Chem.* **1980**, *84*, 3079.
(156) Driscoll, D. J.; Martin, W.; Wang, Ji-W.; Lunsford, J. H. In *Adsorption and Catalysis on Oxide Surfaces*; Che, M., Bond,

G. C., Eds.; Elsevier: Amsterdam, The Netherlands, 1985; p 403.
(157) Che, M.; Tench, A. J. *Adv. Catal.* **1982**, *31*, 77. Che, M.; Tench, A. J. *Adv. Catal.* **1983**, *32*, 1.
(158) Yang, T. J.; Lunsford, J. H. *J. Catal.* **1980**, *63*, 505.
(159) Khan, M. M.; Somorjai, G. A. *J. Catal.* **1985**, *91*, 263.
(160) Liu, H. F.; Liu, R.-S.; Liew, K. Y.; Johnson, R. E.; Lunsford, J. H. *J. Am. Chem. Soc.* **1984**, *106*, 4117.
(161) Ebner, J. R.; Gleaves, J. T. *Proceedings, 5th IUCCP Symposium: Oxygen Complexes and Oxygen Activation by Metal Complexes*, College Station, TX, Mar 1987.
(162) Fricke, R.; Jershekewitz, H.-G.; Lischke, G.; Ohlmann, G. *Z. Anorg. Allg. Chem.* **1979**, *23*, 448.
(163) Busca, G.; Centi, G.; Trifirò, F.; Lorenzelli, V. *J. Phys. Chem.* **1986**, *90*, 1337.
(164) Busca, G.; Centi, G.; Trifirò, F. *J. Am. Chem. Soc.* **1985**, *107*, 7757.
(165) Centi, G.; Trifirò, F. Preprints, ACS Symposium of Division of Petroleum Chemistry, "Hydrocarbon Oxidation", New Orleans Meeting, Sept 1987.
(166) Atkinson, R. *Chem. Rev.* **1985**, *85*, 69.
(167) Puttock, S. J.; Rochester, C. H. *J. Chem. Soc., Faraday Trans. 1* **1986**, *82*, 2773.
(168) Puttock, S. J.; Rochester, C. H. *J. Chem. Soc., Faraday Trans. 1* **1986**, *82*, 3013.
(169) Mars, P.; van Krevelen, D. W. *Chem. Eng. Sci.* (Special Supplement), **1954**, *3*, 41.
(170) Glaeser, L. C.; Brazdil, J. F.; Hazle, M. A.; Mehicic, M.; Grasselli, R. K. *J. Chem. Soc., Faraday Trans. 1* **1985**, *81*, 2903.
(171) Ueda, W.; Moro-oka, Y.; Ikawa, T. *J. Chem. Soc., Faraday Trans. 1* **1982**, *78*, 495.
(172) Shets, V. A.; Sarichev, M. E.; Kazanskii, V. B. *J. Catal.* **1968**, *11*, 378.
(173) Petts, R. W.; Waugh, K. C. *J. Chem. Soc., Faraday Trans. 1* **1982**, *78*, 803.
(174) Weiss, F.; Marion, J.; Metzger, J.; Cognion, J.-M. *Kinet. Catal. (Engl. Transl.)* **1973**, *14*, 32.
(175) Centi, G.; Trifirò, F. *J. Mol. Catal.* **1986**, *35*, 255.
(176) Cavani, F.; Centi, G.; Manenti, I.; Trifirò, F. Italian Patent 20415 A/84, 1984.
(177) Busca, G.; Centi, G.; Trifirò, F. In *Proceedings, 4th International Congress on Catalysts Deactivation* (Antwerp, Belgium, Sept 1987).
(178) Busca, G.; Lavalley, J. C. *Spectrochim. Acta, Part A* **1986**, *42a*, 443.
(179) Puttock, S. J.; Rochester, C. H. *J. Chem. Soc., Faraday Trans. 1* **1986**, *82*, 3033.
(180) Rozhkova, E. V.; Gerei, S. V.; Gorokhovatskii, Ya. B. *Kinet. Catal. (Engl. Transl.)* **1975**, *15*, 618.
(181) Centi, G.; Dyrek, K.; Labanowska, M.; Trifirò, F. In *Proceedings, 31st International Congress on Pure and Applied Chemistry* (Sofia, Bulgaria, July 1987).
(182) Sleight, A. W. In *Advanced Materials in Catalysis*, Burton, J. J., Garten, R. L., Eds.; Academic: New York, 1977; p 181.
(183) Brazdil, J. F.; Teller, R. G.; Grasselli, R. K.; Kostiner, E. In *Solid State Chemistry in Catalysis*; Grasselli, R. K., Brazdil, J. F., Eds.; American Chemical Society: Washington, DC, 1985; p 57 ACS Symp. Ser. 279,
(184) Centi, G.; Trifirò, F. *Catal. Rev.—Sci. Eng.* **1986**, *28*, 165.
(185) Jung, J. S.; Bordes, E.; Courtine, P. In *Adsorption and Catalysis on Oxide Surfaces*; Che, M., Bond, G. C., Eds.; Elsevier: Amsterdam, The Netherlands, 1985; p 334.
(186) Volta, J. C.; Portefaix, J. L. *Appl. Catal.* **1985**, *18*, 1. Ziolkowski, J. *J. Catal.* **1983**, *84*, 74, 317. Germain, J. E. In *Adsorption and Catalysis on Oxide Surfaces*; Che, M., Bond, G. C., Eds.; Elsevier: Amsterdam, The Netherlands, 1985; p 232.
(187) Crabtree, R. H. *Chem. Rev.* **1985**, *85*, 245. Schwartz, J. *Acc. Chem. Res.* **1985**, *18*, 302.
(188) Gesser, H. D.; Hunter, N. R.; Prakash, C. B. *Chem. Rev.* **1985**, *85*, 235. Pitchai, P.; Klier, K. *Catal. Rev.—Sci. Eng.* **1986**, *28*, 13.